Journal of Inflammation Research

Dovepress
Taylor & Francis Group

Open Access Full Text Article

ORIGINAL RESEARCH

A Chimeric Peptide Derived from a Bacterial Effector Protein Attenuates TLR-2/4-Mediated Production of Pro-Inflammatory Cytokines and Enhances the Cellular Availability of Gentamicin

Binita Roy Nandi[1,2], Biswaranjan Patra[1,2], Girish K Radhakrishnan[1]

[1]Laboratory of Bacterial Pathogenesis, National Institute of Animal Biotechnology, Hyderabad, Telangana, 500032, India; [2]Regional Centre for Biotechnology (RCB), Faridabad, 121001, India

Correspondence: Girish K Radhakrishnan, Email girish@niab.org.in

Introduction: Toll-like receptors (TLRs) are critical components of innate immunity, recognizing microbe-derived molecules and triggering pro-inflammatory cytokine production for pathogen clearance. However, TLR hyperactivation can cause excessive inflammation, contributing to disorders such as sepsis. Thus, modulating TLR signalling is a promising therapeutic strategy. The intracellular bacterial pathogen, *Brucella*, encodes TcpB, a cell-permeable anti-inflammatory protein that inhibits TLR2/4 signalling by targeting adaptor proteins TIRAP and MyD88. TcpB has an N-terminal phospholipid-binding motif conferring cell permeability and a C-terminal TIR domain for TLR interference. This study explores TcpB-derived peptides and evaluates their potential for therapeutic and research applications.

Methods: We synthesized TcpB-derived peptides and evaluated their cytotoxicity, cell permeability, and anti-inflammatory effects using LDH assay, fluorescence microscopy, ELISA, and qRT-PCR. A chimeric peptide, TB4-BBL2, was then generated and evaluated for cellular uptake, interaction with TLR adaptors, and functional activities. Binding of FAM-labelled TB4-BBL2 to FLAG-tagged TIRAP/MYD88 was confirmed via co-immunoprecipitation and fluorescence analysis, while degradation of adaptors was assessed by Western blotting. The anti-inflammatory efficacy of TB4-BBL2 was evaluated in a murine endotoxemia model by measuring serum TNF-α and IL-6 levels using ELISA, and cytokine transcript levels in major organs using qRT-PCR. Additionally, TcpB-derived peptides conjugated to gentamicin were analyzed for enhanced intracellular delivery, bacterial clearance, and anti-inflammatory effects using CFU enumeration, ELISA, and qRT-PCR in both in vitro and in vivo.

Results: TB4-BBL2 peptide was efficiently internalized by macrophages via endocytosis and promoted the degradation of TIRAP and MYD88, thereby attenuating TLR2/4-mediated pro-inflammatory cytokine production and oxidative stress. In vivo, TB4-BBL2 treatment resulted in over a 70% reduction in serum TNF-α levels, which was also reflected by decreased transcript levels in spleen tissue. Conjugation of TcpB-derived peptides to gentamicin enhanced its cell permeability and facilitated efficient elimination of intracellular bacteria. This was corroborated by enhanced bacterial clearance in CFU assays, showing over a 2-Log reduction in vivo along with more than an 80% decrease in splenic TNF-α transcripts in the murine model of brucellosis.

Discussion: Our findings highlight the therapeutic potential of TcpB-derived peptides in modulating TLR-mediated inflammation and enhancing intracellular antibiotic delivery. This dual-functional strategy offers a promising novel approach for treating inflammatory diseases and persistent intracellular infections, warranting further investigation toward clinical applications.

Keywords: inflammation, TLR2/4, pro-inflammatory cytokines, inflammatory disorders, peptide-based drugs, *Brucella*, endotoxemia, cell-permeable antibiotics

Introduction

Toll-like receptors are crucial components of innate immunity, which is the first line of defence against invaded microorganisms. TLRs are expressed in a wide range of host cells, including macrophages, dendritic cells, B cells,

Received: 1 April 2025
Accepted: 5 July 2025
Published: 9 August 2025

Graphical Abstract

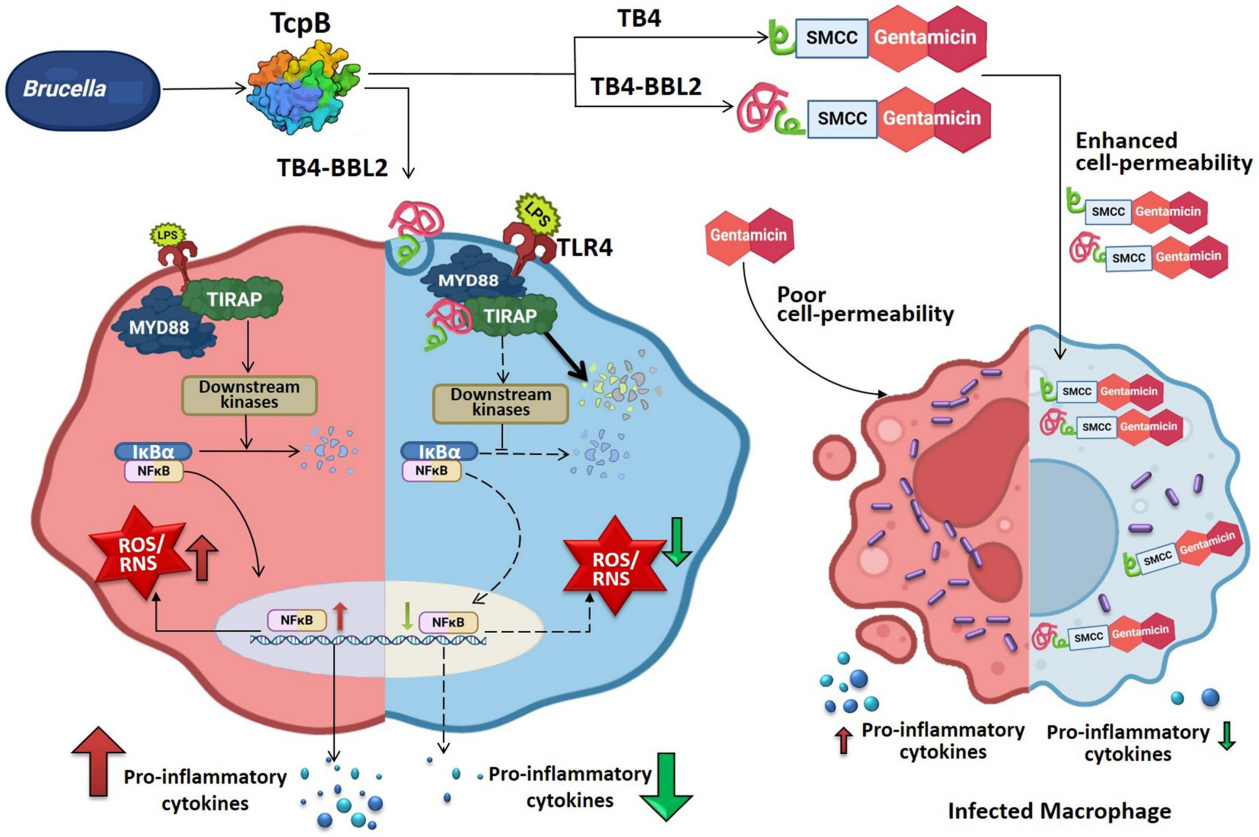

epithelial and fibroblast cells. TLRs constitute an extracellular leucine-rich repeat (LRRs) that are involved in recognizing various pathogen-associated molecular patterns (PAMPs). TLRs harbour an intracellular domain termed the TIR domain, which is highly conserved and interacts with the TIR domain-containing adaptor proteins upon activation. There are four TIR domain-containing adaptor proteins such as TIRAP (TIR-domain-containing adaptor protein (TIRAP), Myeloid differentiation primary response protein 88 (MyD88), TIR domain-containing adaptor protein inducing interferon-β (TRIF) and TRIF-related adaptor molecule (TRAM) that are involved in the initiation of TLR signalling.[1] The recognition of PAMPs by the TLRs triggers their activation, followed by selective recruitment of the TIR domain-containing adaptor proteins. This initiates a signalling cascade that results in expression of various pro-inflammatory cytokines, chemokines and anti-microbial peptides.[2]

Dysregulated TLR activation can produce excess pro-inflammatory cytokines, resulting in whole-body inflammation. The aberrant activation of TLRs has been attributed to the pathogenesis of various inflammatory disorders, including sepsis, atherosclerosis, diabetes, and arthritis.[3,4] The dysregulated activation of TLR4/2 by PAMPs results in excess production of pro-inflammatory cytokines, free radicals, and recruitment of other inflammatory mediators, leading to a systemic syndrome with tissue injury, increased vascular permeability, and multi-organ failure.[5,6] TLR4 and TLR2 play crucial roles in the pathogenesis of inflammatory disorders like sepsis, making them promising therapeutic targets. However, no specific drugs are currently approved for sepsis treatment. Moreover, antibacterial therapy can worsen inflammation by releasing PAMPs that activate TLR4 and 2. While immunosuppressive agents like steroids can reduce systemic inflammation, their long-term use leads to severe side effects and heightened susceptibility to secondary or opportunistic infections.[7]

Many pathogenic microorganisms encode effector proteins that subvert the TLR signalling to attenuate the production of pro-inflammatory cytokines.[8] Bacterial pathogens such as *Brucella, Salmonella, E. coli* etc. encode effector proteins that mimic the TIR domain of eukaryotes to interfere with the TLR signalling.[9,10] TcpB is a cell-permeable, TIR domain-containing protein from the intracellular bacterial pathogen *Brucella*, which inhibits NF-κB activation and the production of proinflammatory cytokines mediated by TLR2 and TLR4.[11–13] The cell permeability of TcpB is attributed to its cationic amino acid-rich N-terminal phosphoinositide phosphate (PIP)-binding motif. Mutation of key residues within this motif significantly reduced the affinity of TcpB for PIPs.[14] The C-terminal TIR domain of TcpB is responsible for disrupting TLR2/4 signalling, thereby downregulating the production of pro-inflammatory cytokines. The BB-loop region in the TIR domain of TcpB has been reported to be essential for interfering with the TLR2/4-mediated signalling pathway.[14] TcpB interacts with the TLR2/4 adaptor proteins, MyD88 and TIRAP and promotes the enhanced ubiquitination and degradation of TIRAP.[10,12,14,15] Although TcpB does not possess inherent ubiquitin ligase activity, it has been shown to interact with the host protein CLIP170, which facilitates the ubiquitination and subsequent degradation of TIRAP.[16] Collectively, these findings suggest that TcpB may serve as a promising candidate for the development of peptide-based, cell-permeable therapeutics targeting TLR2/4 signalling.

Therapeutic proteins are widely used to treat human diseases but face challenges such as immunogenicity and proteolytic instability. To overcome these limitations, peptide sequences are being explored as alternatives, gaining significant interest in the pharmaceutical industry.[17,18] Peptide drugs exhibit enhanced potency, specificity, and low incidence of toxicity.[19,20] Further, the conjugation of peptides with other drugs can improve the target selectivity and bioavailability and facilitate the delivery of cell impermeable cytosolic cargos.[21–24] Therefore, peptide mimetics became one of the thrust areas of drug discovery with unprecedented potential.

The unregulated use of antibiotics has led to the rapid emergence of antibiotic-resistant bacteria, significantly impacting global health. Treating intracellular bacterial infections poses a particular challenge due to the limited cellular availability of antibiotics at therapeutic doses.[25] Given that the discovery of new antibiotics is both time-consuming and financially demanding, alternative strategies are urgently required to combat antimicrobial resistance.[26,27] A promising approach involves modifying existing antibiotics to enhance their pharmacokinetic properties.[18,24]

In this study we generated functional peptides from the TcpB protein of *Brucella*, followed by analysing their cell permeability and anti-inflammatory properties. The chimeric peptide, TB4-BBL2 targeted TIRAP and MYD88 to disrupt TLR2/4 signaling and significantly dampened cytokine induction in a mouse model of endotoxemia. Furthermore, we demonstrated that conjugating gentamicin with the peptides derived from TcpB enhanced its cellular availability, resulting in improved permeability, increased killing of intracellular bacteria, and suppression of proinflammatory cytokines in both macrophages and mice.

Materials and Methods

Sequence Analysis

The TIR domain of TcpB was aligned with that of mouse TIRAP, using the Clustal Omega to identify the BB loop region of TcpB. The crystal structures of TIR domains of TcpB (pdb_00004c7m) and TIRAP (pdb_00002y92) were obtained from PDB and superimposed using Chimaera software.[28,29]

Designing and Synthesis of Peptides from TcpB

Various peptides were designed from the N-terminal PIP-binding and C-terminal BB-loop regions of TcpB (Table 1). The peptides were synthesised without or with a 5-carboxyfluorescein (FAM) tag at the N-terminus from commercial sources with >95% purity by HPLC. The lyophilized peptides were resuspended in 1X DPBS (Lonza) and stored in aliquots in the −80 freezer for further experiments.

Cell Culture

RAW264.7 (ATCC), HEK293T (ATCC) and immortalized Bone Marrow-Derived Macrophages from mice (iBMDM; a gift from Petr Broz, University of Lausanne) were cultured in Dulbecco's Modified Eagle Medium (DMEM, Sigma)

Table 1 Details of Peptides Used in the Study

Peptide	Sequence	Length	Description
TB1	GAAIGKKRADIAKK	14	Derived from N-terminus
TB2	KKRADIAKK	9	Derived from N-terminus
TB2 (ala) (mutated)	AAAADIAAA	9	In TB2, Lys and Arg are replaced with Ala
TB3	GAAIGKKRADIAKKIADKAK	20	Derived from N-terminus
TB4	KKRDIKK	7	Derived from N-terminus
TB5	KKRDKK	6	Derived from N-terminus
TB6	KKRKK	5	Derived from N-terminus
TB7	GKKRADIAKK	10	Derived from N-terminus
TAT	GRKKRRQRRRPPQ	13	Positive control [25]
TAT-ala (-ve control)	GRKKAAQAAAPPQ	13	Negative control [25]
TB4-BBL	KKRDIKKKIFYDAYTLKVGDSLRRKID	27	TB4 with BB loop region of TcpB
TB4-BX2	KKRDIKKLQLRDATPGGAIVS	21	TB4 with BB loop of TIRAP
TBX2	GKMADWFRQTLLKKPKKRPNSPEST LQLRDATPGGAIVS	39	Positive control [25]
TB4-BBL1	KKRDIKKLGAKIFYDAYTLKVGD	23	TB4 with shortened BB loop of TcpB
TB4-BBL2	KKRDIKKRDLGAKIFYDAYTLKVGDSLRR	29	TB4 with extended BB loop of TcpB
TB4-DD	KKRDIKKHKVSYDEVRRFSPSLA	23	TB4 with shortened DD loop of TcpB
TIR	SEDKEAFVQDLVAALRDLGAKIFYDAYTLKVGDSLRRKIDQGLANSK	47	Derived from the TIR domain of TcpB

supplemented with 10% Fetal Bovine Serum (FBS, Sigma) and 1% penicillin-streptomycin solution at 37°C in the humidified atmosphere of 5% CO2. The iBMDMs were differentiated using m-CSF (20 ng/mL; Biolegend) or 10% culture supernatant of L929 cells for 48 hours and further maintained in Dulbecco's Modified Eagle Medium supplemented with 10% Fetal Bovine Serum (FBS, Sigma) and 1% penicillin-streptomycin solution at 37°C.[30]

Fluorescence Microscopy Analysis of Peptide-Treated Cells

RAW264.7 cells (50,000 cells) were seeded into glass bottom petri plates (Eppendorf) or 24-well plates (50,000 cells/wells) and allowed to adhere overnight. Cells were then treated with 100 μM of FAM-labelled peptides for 2 hours. Subsequently, the cells were washed twice with 1X DPBS and treated with 0.1% of Trypsin EDTA (Sigma) for 5 minutes at 37°C to remove extracellular and membrane-bound peptides. Cells were then washed twice with 1X DPBS, followed by fixing the cells with 4% paraformaldehyde in PBS for 20 minutes at room temperature. Next, the nuclei of the cells were stained with Hoechst (Thermo Fisher Scientific) and plates were analysed using a fluorescent microscope (Carl Zeiss) at 20 X magnification. For confocal microscopy, the fixed cells were mounted in Prolong Gold anti-fading agent with DAPI (Thermo Fisher Scientific) and the cells were analysed using a laser confocal microscope (Leica) at 63x magnification. A total of 15 representative fields per sample were examined to assess peptide internalization.

Flow Cytometry Analysis of Peptide-Treated Cells

RAW264.7 cells were seeded into a 12-well plate (75,000 cells/well) and allowed to adhere overnight. Next, the cells were treated with FAM-labelled peptides for 2 hours, followed by treatment with 0.1% Trypsin-EDTA for 5 minutes at 37°C to remove the extracellular peptides. Subsequently the cells were washed with 1X DPBS and fixed with 4% paraformaldehyde as described before. The cells were collected and resuspended in 500 μL of ice-cold 1X PBS supplemented with 0.05% trypan blue (Sigma), followed by quantifying the fluorescence using flow cytometry (BD Fortessa). A total of 50,000 events

were acquired and examined per sample using BD Fortessa flow cytometer. The data were analyzed using FlowJo software (BD Biosciences). Mean fluorescence intensity (MFI) of FAM signal was calculated to quantify peptide internalization. Statistical significance between groups was determined using one-way ANOVA.

Peptide Internalization Assays with Inhibitors

To perform the cold inhibition, RAW264.7 cells (50,000 cells) were seeded into glass bottom petri plates and allowed to adhere overnight. The cells were then treated with 50 μM of FAM-labelled peptides at 4°C for 2 hours, followed by processing the cells for microscopy and flow cytometry analysis as described before. To perform chemical inhibition, RAW264.7 cells were treated with indicated concentrations of various inhibitors such as Nocodazole (blocks microtubule polymerization, Sigma), Wortmannin (inhibitor of phosphoinositide 3-kinase involved in transcytosis, Sigma), methylated-β-cyclodextrin (MβCD, a caveolae-mediated endocytosis inhibitor by depleting cholesterol, Sigma), Cytochalasin D (inhibits macropinocytosis, Sigma), and Chlorpromazine (inhibits clathrin-mediated endocytosis, Sigma) for 30 minutes at 37°C, followed by treatment with FAM-labelled peptides (50 μM) for 2 hours. The cells were then processed for microscopy and flow cytometry analysis as described before.

Peptide Treatment and Stimulation of Macrophages with LPS

RAW264.7 or iBMDMs were seeded in 24-well plates (50,000 cells/well) and allowed to adhere overnight. Cells were then treated with various concentrations of peptides for 1 hour, followed by stimulation of cells with Lipopolysaccharide (LPS, 200 ng/mL, Sigma). The cells or culture supernatants were harvested at various times post-LPS stimulation, followed by quantification of TNF-α and IL-6 levels using qRT-PCR and ELISA.

Quantification of Pro-Inflammatory Cytokines

The mRNA levels of pro-inflammatory cytokines in cells or harvested mice organs were examined by isolating the total RNA and performing qRT-PCR. Briefly, cells or mice organs (spleen, liver, lungs, and kidneys) were harvested and homogenized in RNAiso PLUS (Takara), followed by total RNA extraction and cDNA synthesis using the Prime Script™ RT Reagent kit (Takara) according to the manufacturer's instructions. Next, the qRT-PCR was performed using the primers specific for TNF-α, IL-6, and GAPDH. The relative gene expression was determined using the comparative $2^{-\Delta\Delta Ct}$ method using CFX Maestro Software (Bio-Rad). Data were normalized with the endogenous control, GAPDH.

To quantify pro-inflammatory cytokines in the serum, blood was collected from mice by cardiac puncture, followed by separation of the serum. The levels of TNF-α and IL-6 in serum or culture supernatants were quantified using the DuoSet ELISA kit (R&D Systems), following the manufacturer's protocol.

Quantification of the Secreted Lactate Dehydrogenase (LDH)

To examine cytotoxicity through quantifying the secreted LDH, immortalised BMDM cells were seeded into 24-well plates and allowed to adhere overnight. The cells were then treated with indicated concentrations of various inhibitors or peptides, and the supernatants were harvested at 5 hours post-treatment. The secreted LDH in the culture supernatants was quantified using the LDH Cytotoxicity detection kit (Takara Bio) as per the manufacturer's instructions. The clarified supernatant obtained from cells lysed with 0.1% Triton X 100 was used as the positive control.

NF-κB Reporter Assay

RAW264.7 cells were seeded into a 12-well plate (75,000 cells/well) and allowed to adhere overnight. Cells were then transfected with pLuc-NF-κB (1 μg/well, Stratagene) and pRL-TK (200 ng/well, Promega) using Xfect transfection reagent (Takara Bio) according to the manufacturer's instructions. Twenty-four hours post-transfection, cells were treated with increasing concentrations of TB4-BBL2 peptide, followed by induction with LPS for 5 hours. Subsequently, the cells were lysed with 1X Passive Lysis Buffer at 4°C for 30 minutes, followed by clarification of the lysate by centrifugation. Firefly and Renilla luciferase activities were then quantified using the Dual-Luciferase Reporter Assay System (Promega), according to the manufacturer's instructions. Firefly luminescence was normalized to Renilla luminescence, and the data were expressed as the fold change in NF-κB activation between LPS-stimulated and unstimulated cells.

Detection of Reactive Oxygen Species (ROS) and Nitric Oxide (NO) in TB4-BBL2-Treated Mouse Macrophages

RAW264.7 cells were seeded in a 12-well plate (75,000 cells/well) in phenol red-free DMEM supplemented with 10% FBS and 1% penicillin-streptomycin solution and allowed to adhere overnight. The cells were treated with TB4-BBL2 for 1 hour, followed by LPS induction (200 ng/mL) for twenty-four hours. Subsequently, the culture supernatant was collected, and the level of NO was measured using the Griess assay kit (Invitrogen) as per the manufacturer's instruction. To examine the level of ROS, the cells were treated with the membrane-permeable redox-sensitive probe, 2′,7′-dicholorodihydroxyfluroscein diacetate (H_2DCFDA) (10 μM, Invitrogen) for 30 minutes at 37°C. Next, the cells were washed thrice with 1X PBS and analyzed immediately for DCF formation using the multimode reader (PerkinElmer) with excitation at 495 nm and emission at 517 nm.

Co-Immunoprecipitation Experiments

HEK293T (1 X 10^6) cells were transfected with FLAG-TIRAP/ MYD88/ USP8/ EV with the Turbofect reagent (Thermo Fisher Scientific). The FLAG-tagged empty vector (EV) was used as a negative control, as it does not express any fusion protein capable of specifically interacting with the FAM-labelled peptides, thereby providing a measure of non-specific background fluorescence. Twenty-four hours post transfections, cells were lysed in the lysis buffer containing 20 mM Tris [pH 8.0], 150 mM NaCl, 1% Triton X100, 1 mM EDTA and 1X protease inhibitor cocktail (Pierce) at 4°C for 20 minutes. The lysates were clarified by centrifugation at 12,000 rpm for 20 min at 4°C. Next, the lysates were incubated with 50 μM of FAM-labelled TB4/TAT/TB4-BBL2 for 4 hours on a rotator at 4°C. Subsequently, 5 μg of anti-FLAG antibody (Sigma) was added to the lysates and incubated overnight at 4°C on the rotator. Next, the lysates were mixed with protein G plus agarose beads (Santa Cruz Biotechnology) and incubated for 2 hours at 4°C. Subsequently, agarose beads were washed three times with 1X IP buffer (20 mM Tris [pH8.0], 150 mM NaCl, 1% Triton X100) and re-suspended in 200 μL of 1X PBS. The samples were then transferred to 96-well Optiplate (PerkinElmer) and the fluorescence intensity was measured using the multimode reader (PerkinElmer) at an excitation of 490 nm and the emission at 520 nm.

Microscale Thermophoresis (MST) Analysis

To examine the interaction between TIRAP and TB4-BBL2 peptide using MST, we cloned and expressed murine TIRAP in *E. coli* as a fusion protein with maltose-binding protein (MBP). Subsequently, the recombinant MBP-TIRAP was purified in native condition using amylose affinity chromatography. The interaction between MBP-TIRAP and the FAM-labelled TB4-BBL2 was then examined using MST. The constant amount (100 nM) of FAM-labeled TB4-BBL2 was mixed with the increasing concentrations of MBP-TIRAP or MBP alone (0.0153 nM to 500 nM) in 1X DPBS (Sigma) containing 0.05% Tween-20. Ten minutes post-incubation at room temperature, the samples were loaded into Monolith™ standard-treated capillaries (Monolith TM NT.115 hydrophilic capillaries). MBP alone was used as the negative control (non-binder). During the experiment, the LED power of the instrument was kept at 40%, and MST power was maintained at a medium level. The binding experiments were performed in triplicate (n = 3 independent replicates), and the binding curve was obtained at 25°C using Monolith NT.115 instrument (NanoTemper Technologies). The Kd value was fitted using MO. Affinity analysis was performed using Affinity Analysis software (NanoTemper Technologies) and the final Kd value is reported as the mean ± standard deviation (SD).

Detection of Protein Degradation by Immunoblotting

RAW264.7 cells were seeded in a 12-well plate (75,000 cells/well) and allowed to adhere overnight. The cells were treated with 10 and 50 μM of TB4-BBL2 peptide and 50 μM of TIR peptide (cell-impermeable) for 5 hours. Subsequently, the cells were washed with ice-cold 1X DPBS and treated with 0.1% Trypsin-EDTA for 5 minutes at 37°C. Cells were washed again with 1X DPBS, followed by lysing the cells in radioimmunoprecipitation assay buffer (RIPA; 10 mM Tris HCL pH 8, 1mM EDTA, 1% Triton X 100, 0.1% SDS, 40 mM NaCl) with the protease inhibitor cocktail (Pierce). The lysate was processed for immunoblotting as described previously.[31] The immunoblots were probed

with primary antibodies against TIRAP, MYD88, TLR2 (1:2000; Cell Signaling Technology), and TRIF (1:1000; Santa Cruz Biotechnology), followed by incubation with an HRP-conjugated secondary antibody.

Pulse-Chase Analysis

To perform pulse-chase analysis with cycloheximide, RAW264.7 cells were treated with TB4-BBL2 for 3 hours and washed with 1X DPBS. Next, the cells were treated with cycloheximide (1 mg/mL; Sigma), followed by harvesting the cells at 1-, 2-, and 3-hours post-treatment. The cells were then lysed and subjected to immunoblotting, as described before.

Dosage Tolerance Experiments with the TB4-BBL2 Peptide

To determine the dosage tolerance, 15 male BALB/c mice were divided into 5 groups (3 mice/group) according to the dosages (5, 10, 20, and 40 mg/kg) of the TB4-BBL2 peptide, and PBS alone was used as the vehicle control. The mice were injected intravenously with the indicated doses of TB4-BBL2 peptide in sterile PBS and observed for toxicity indicators until 5 days post-injection, where the parameters were recorded every 6 hours. After 5 days, blood and organs were harvested from mice for detailed examination. Serum was separated from blood and analysed for pro-inflammatory cytokine levels using ELISA as described before.

Induction of Endotoxemia in Mice and Analysing the Effect of TB4-BBL2 Peptide

To optimise the dosage and analyse the effect of pre-treatment with TB4-BBL2 peptide, 25 mice were randomly distributed into 5 groups (5 mice/group) according to the dosages and controls (20, 30 and 40 mg/kg; PBS+LPS and PBS alone). Next, the mice were injected intravenously with the indicated concentrations of TB4-BBL2 peptide. One hour later, mice were injected intraperitoneally with *E. coli* LPS (25 mg/kg; Sigma). Two hours post-LPS treatment, blood was collected from the mice through the cardiac puncture, followed by euthanizing the mice and harvesting of the liver, spleen, kidney, and lungs. Serum was separated from the collected blood and the levels of pro-inflammatory cytokines in the serum and organs were quantified by ELISA and qRT-PCR, respectively, as described before.

To analyse the effect of post-treatment with TB4-BBL2, 15 mice (5 mice/group) were randomly distributed into 3 groups (PBS, PBS+LPS and TB4-BBL2 peptide+LPS). Next, the mice were treated intraperitoneally with *E. coli* LPS (25 mg/kg) for 1 hour, followed by administration of TB4-BBL2 peptide (30 mg/kg). The mice were sacrificed 2 hours post-TB4-BBL2 peptide delivery, and the samples were harvested and processed as described before.

To analyse the effect of simultaneous administration of LPS and TB4-BBL2, 15 mice (5 mice/group) were randomly distributed into 3 groups (PBS, PBS+LPS and 30 mg/kg of TB4-BBL2 peptide+LPS). The mice were administered with LPS (25 mg/kg) intraperitoneally, followed by treatment with TB4-BBL2 peptide (30 mg/kg) intravenously. The mice were sacrificed 3 hours post-injections, and the samples were harvested and processed as described before.

Histopathology Studies

The liver, lungs, kidneys, and spleen were harvested from peptide/LPS-treated mice and fixed with 10% neutral buffer saline for 24 hours. The tissues were processed for dehydration, clearing, and impregnation using isopropanol gradients and xylene. The tissues were then embedded in parafilm blocks, followed by cutting sections using a microtome (Leica microtome). The tissue sections were stained with haematoxylin and eosin dyes (Sigma) and analysed using a light microscope (Zeiss).

Conjugation of Gentamicin with cTB4 or cTB4-BBL2

cTB4 or cTB4-BBL2 (peptides with cysteine at the N-terminus) were synthesized and conjugated with the broad-spectrum antibiotic, gentamicin, using SMCC as the cross-linker, to generate gentamicin-conjugated cTB4 (cTB4-G) and gentamicin conjugated cTB4-BBL2 (cTB4-BBL2-G). SMCC forms stable amide bonds with the gentamicin amino group and stable thioether bonds with the N-terminal thiol group in cTB4 or cTB4-BBL2, thereby facilitating gentamicin peptide conjugation. SMCC was dissolved in DMSO at a concentration of 25 mg/mL to prepare a stock solution. It was then diluted to the appropriate concentrations and incubated with gentamicin in PBS, used as the conjugation buffer, at room temperature for two hours. Subsequently, peptides were added to the solution and incubated for two more hours at room temperature. To estimate the percentage of conjugation through free thiol group estimation, DTNB/ Ellman's reagent was used.

Estimation of Free Thiol Group

Conjugated and unconjugated cTB4 were serially diluted and incubated with the Ellman's reagent (DNTB) for 30 minutes at room temperature in a microtiter plate. After incubation, the absorbance was measured at 412 nm. The DNTB detects the free sulfhydryl groups (thiols) in a solution. DNTB reacts with free thiol groups (-SH) to form a mixed disulfide and 5-thio-2-nitrobenzoic acid (TNB), which can be quantified at 412 nm. Consequently, a higher absorbance value at 412 nm indicates a greater presence of free thiol groups in unconjugated cTB4. In contrast, a lower optical density at 412 nm suggests effective conjugation between cTB4 and the SMCC-linked Gentamicin.

Gentamicin Efficiency Assay

To assess the bactericidal efficiency of conjugated gentamicin, a gentamicin efficiency assay was performed following the method of Gomarasca et al, (2017). Primary cultures of *B. neotomae* and *S. typhimurium* were diluted at ratios of 1:5 and 1:100, respectively, in fresh growth medium, followed by the addition of gentamicin-cTB4 conjugate (cTB4-G). As controls, individual components of the conjugation reaction were added, such as gentamicin (50 μg/mL), DMSO (15 μL), and SMCC (150 μg/mL). The optical density of the bacterial cultures was recorded at OD_{600} after 4 and 16 hours of treatment to monitor the bacterial growth. To evaluate the antibacterial properties of the conjugates in vitro, macrophages were infected with *Brucella* or *Salmonella* and subsequently treated with either controls or conjugates at the indicated time points. Following treatment, the macrophages were lysed, and intracellular bacterial loads were quantified by CFU assays.

To Examine the Effect of cTB4-BBL2-Gentamicin Conjugate in Mice Infected with *B. melitensis*

To evaluate the in vivo effect of cTB4-BBL2-Gentamicin in the *B. melitensis* infected mice, 8-week-old female BALB/c mice (6 mice per group) were infected intraperitoneally with *B. melitensis* (2×10^5 CFU per mouse) in 100 μL of 1X PBS. Ten days post-infection, each infected mouse was treated intraperitoneally with one of the following: PBS, gentamicin (0.2 mg), cTB4-G (0.2 mg gentamicin conjugated with 0.4 mg of cTB4 using 0.4 mg of SMCC), or cTB4-BBL2-G (0.2 mg gentamicin conjugated with 0.4 mg of cTB4-BBL2 using 0.4 mg of SMCC) for 3 consecutive days. Fourteen days post-infection, blood was collected from the mice through cardiac puncture, followed by euthanizing the mice, harvesting the organs, and CFU analysis to quantify the splenic load of *B. melitensis*. Serum was isolated from blood to quantify secretedTNF-α levels by ELISA. The quantification of mRNA levels of TNF-α and IL-6 in the spleen, liver, kidney, and lungs was carried out through qRT-PCR as previously described.

Ethical Statement

Six to eight-week-old BALB/c mice (20–25 g) were obtained from and housed at the small animal experimentation facility of the National Institute of Animal Biotechnology (NIAB), Hyderabad, with food and water ad libitum. The experimental protocols were approved by the Institutional Biosafety Committee (Approval number: IBSC/Jul2020/NIAB/GR01) and Institutional Animal Ethics Committee (Approval number: IAEC/2019/NIAB/35/GKR). All procedures were conducted in accordance with the guidelines of the Committee for Control and Supervision of Experiments on Animals (CCSEA), Government of India, for the care and use of laboratory animals.

Statistical Analysis

The GraphPad Prism 6.0 software was used for statistical analysis of experimental data. Data are represented with the mean ± standard deviation (SD) or standard error of the mean (SEM) as mentioned in respective figure legends. For pairwise comparison, statistical significance was determined by unpaired t-tests (two-tailed). A one-way analysis of variance (ANOVA) test was used to analyse the statistical significance of data including more than two samples. A p-value less than 0.05 ($p < 0.05$) was considered statistically significant. The significance levels were indicated as follows: n.s. (not significant), $p > 0.05$; *: $p < 0.05$; **: $p < 0.01$; ***: $p < 0.001$; ****: $p < 0.0001$. All experiments were performed independently at least three times.

Results

Designing of Cell-Permeable and Anti-Inflammatory Peptides from TcpB Protein

TcpB protein consists of an N-terminal PIP-binding motif and a TIR domain at its C-terminus (Figure 1A). The PIP-binding motif is rich in arginine and lysine residues, which is reported to bind to many species of PIPs.[14] The association of TcpB with the plasma membrane and its internalization by macrophages has been previously reported.[11,14] Furthermore, the membrane binding property of TcpB was attributed to its N-terminal fragment.[11,14] Considering these facts, we sought to identify the shortest peptide, which confers the cell-permeability of TcpB. To achieve this, we designed various peptides from the N-terminal PIP-binding motif of TcpB and synthesised the peptides with the FAM label at their N-terminus (Table 1). The TIR domain of TcpB interferes with the TLR2/4 signalling where the BB-loop region is essential for this activity.[14] The TIR domain of TcpB shares considerable amino acid similarity to that of other TIR domain-containing eukaryotic proteins, including the TLR2/4 adaptor protein, TIRAP. To identify the exact region of BB-loop in the TcpB, we aligned the TIR domain sequences of TcpB and TIRAP (Figure 1B). In agreement with the sequence similarity, the BB-loop of TcpB and TIRAP exhibited high structural superimposition (Figure 1C–E). Next, we designed peptides from the BB-loop region of TcpB for further studies (Table 1).

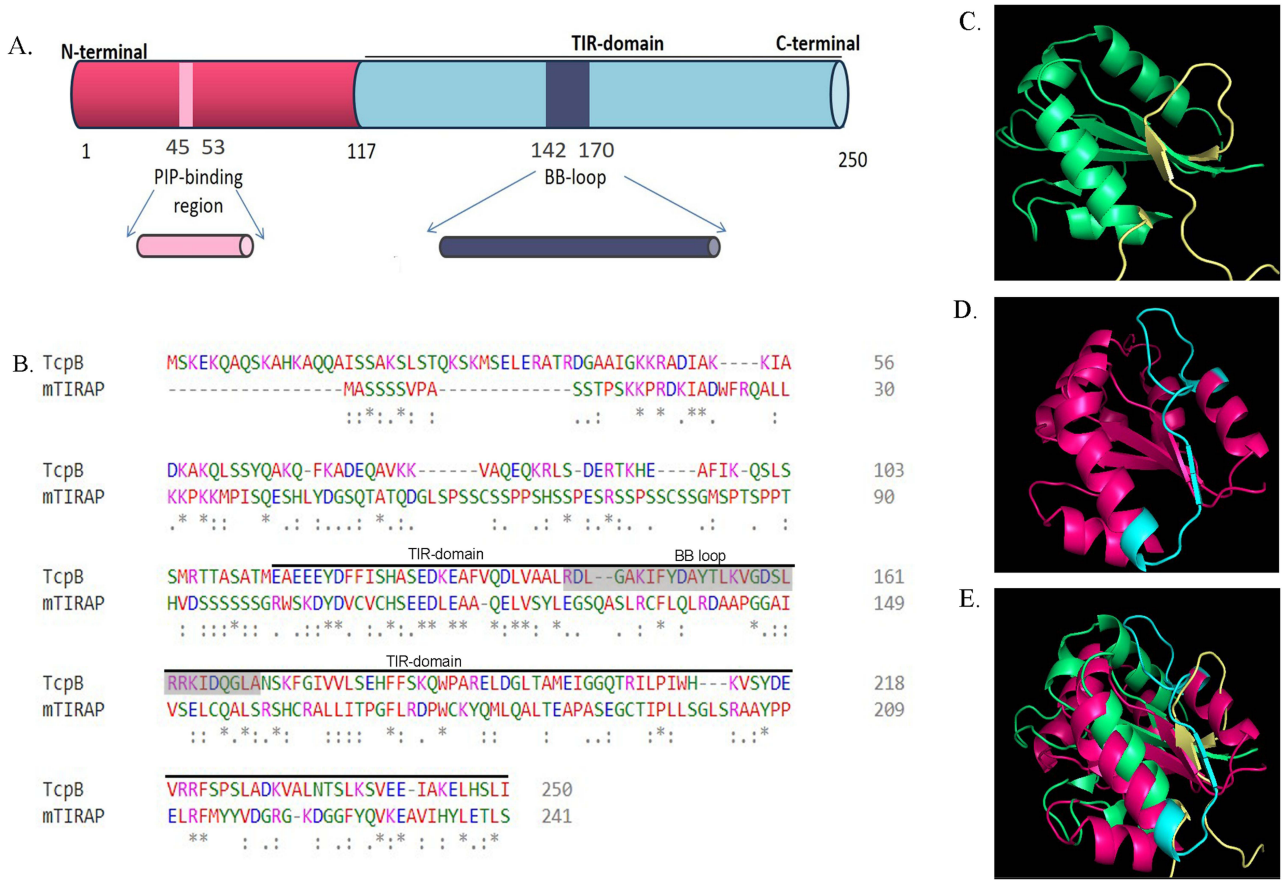

Figure 1 BB loop in the TIR domain of TcpB and TIRAP share multiple conserved residues. (**A**) A schematic illustration of domain structure of TcpB protein. TcpB harbours an N-terminal PIP-binding motif and C-terminal TIR domain with the BB-loop. (**B**) Pair-wise sequence alignment showing the conserved amino acid residues among the TIR domain of TcpB and TIRAP (mouse). (**C** and **D**) Ribbon diagram showing the BB-loop region of TcpB (blue) and TIRAP (yellow) in the TIR domain. (**E**) Structural superimposition of TIR domain of TcpB and TIRAP showing the alignment of the BB-loop.

https://doi.org/10.2147/JIR.S526902

Peptide from the PIP-Binding Motif of TcpB is Cell Permeable and Internalized Through Cholesterol-Dependent Endocytosis

We synthesized peptides from the PIP-binding motif of TcpB with FAM label to examine their internalization using fluorescent microscopy and flow cytometry. RAW264.7 mouse macrophage cell lines were treated with 100 μM of FAM-labelled peptides, followed by fixing the cells and analysing them using laser confocal microscopy and flow cytometry. The peptide derived from the TAT protein of HIV and its mutant version, where lysine and arginine residues were mutated to Alanine (TATala), were used as the positive and negative controls, respectively.[32] The confocal microscopy analyses showed the accumulation of TcpB-derived peptides, designated here as TB1, TB2, TB3, and TB4, in the macrophages as efficiently as the positive control, TAT peptide (Figure 2A). The truncated versions of the TB4 peptide *viz*. TB5, TB6, and TB7 peptides showed diminished cell permeability compared to TB4 (Figure 2A and B). Subsequently, we performed a flow cytometry analysis of peptide-treated macrophages that also showed the internalization of TB4 as effective as TAT peptide (Figure 2B). Further, we observed that the replacement of lysine residues with alanine in the cell-permeable peptide affected its uptake as the mutant version of the TB2 (TB2ala) peptide failed to accumulate in the treated macrophages (Figure 2A). Based on the peptide internalization studies, the TB4 peptide with 7 amino acids was the shortest peptide derived from TcpB, displaying efficient cell permeability. Subsequently, we analysed the permeability of TB4 in various cell types. TB4 was efficiently internalised by N9 microglial cells and human monocyte-derived macrophages (THP1) (Appendix Figure S1A). We did not observe internalization of the TB4 peptide by the human embryonic kidney cell line, HEK293 (Appendix Figure S1A).

Next, we sought to examine the mechanism by which macrophages internalise the TB4 peptide. The accumulation of TB4 was affected when the peptide uptake assay was performed at 4°C, indicating that internalization of TB4 peptide occurs through ATP-dependent endocytosis and not through passive translocation (Figure 2C). To examine the mechanism of internalization, we treated cells with various compounds that inhibit cellular uptake of macromolecules through endocytosis. The cytotoxicity of the compounds was examined to determine the treatment dose of inhibitors (Appendix Figure S1B). Treatment of cells with wortmannin (inhibitor of phosphoinositide 3-kinase mediated transcytosis), cytochalasin D (inhibits micropinocytosis), chlorpromazine (inhibits clathrin-mediated endocytosis) did not impact the uptake of TB4 (Figure 2C). In contrast, treatment of cells with nocodazole (blocks microtubule polymerization) and methylated-β-cyclodextrin (inhibits caveolae-mediated endocytosis through cholesterol depletion) affected the uptake of TB4 peptide by macrophages (Figure 2C and D). To corroborate these findings, we treated cells with increasing concentrations of methylated-β-cyclodextrin or nocodazole, followed by analysing the uptake of the TB4 peptide. We observed a dose-dependent inhibition of TB4 internalization by the compound-treated macrophages (Figure 2E and F). Collectively, our experimental data indicate that the cells internalize TB4 peptide through active endocytosis that requires cholesterol-rich lipid rafts.

Generation of a Chimeric Peptide with Cell Permeability and Anti-Inflammatory Properties

The TIR domain and intact BB loop are required for the anti-inflammatory property of TcpB.[33] To verify this, we overexpressed the TIR domain of TcpB in macrophages, followed by analyzing its efficiency in suppressing LPS-induced pro-inflammatory cytokines. RAW264.7 cells were transfected with the TIR domain of TcpB, followed by treatment of cells with LPS. We observed suppression of LPS-induced production of pro-inflammatory cytokines, TNF-α, and IL-6 in the macrophages transfected with the TIR domain of TcpB (Figure 3A and B). Next, we designed peptides from the BB-loop region of TcpB, designated as BBL, and fused them with the cell-permeable peptide TB4 at the N-terminus (TB4-BBL). The TB4-BBL peptide carried the entire BB loop region of TcpB (Table 1). We also generated TB4-BBL1, which carried a shorter BB-loop, and TB4-BBL2 with an extended BB-loop region (Appendix Figure S2A). We synthesized two control peptides *viz*. TBX2, the cell-permeable anti-inflammatory peptide from TIRAP and TB4-BX2 where the anti-inflammatory peptide from TIRAP has been fused with the TB4 peptide.[32] Next, we analysed the cell permeability of TcpB and TIRAP-derived peptides and all the peptides were efficiently internalized by the macrophages (Appendix Figure S2B). To examine, whether the peptides induce any cytotoxicity, iBMDMs were treated with cell-permeable

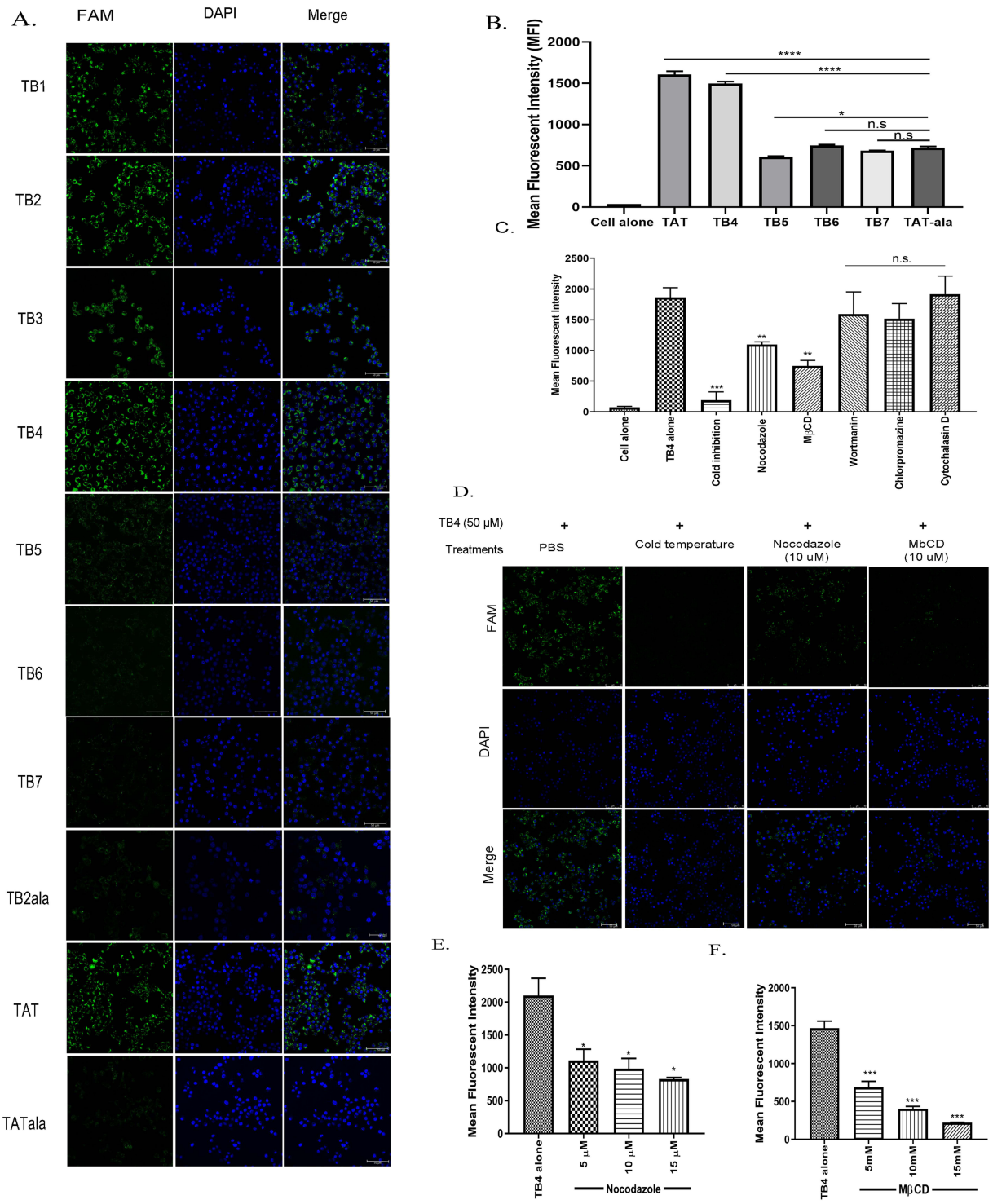

Figure 2 Generation of cell permeable peptides from the PIP-binding motif of TcpB (**A**) Uptake of TcpB derived peptides by macrophages. RAW264.7 cells were treated with FAM-labelled peptides from the PIP-binding motif of TcpB for 2 hours, followed by processing the cells for fluorescent microscopy. The green fluorescence inside the cells shows the internalised peptides and the nuclei stained with DAPI (blue). The cells were imaged using a laser confocal microscope at 63×. Scale bar, 50 μm. Image represents 10 different fields captured from cells treated with peptide. (**B**) Quantification of internalized peptides in RAW264.7 cells by flow cytometry. Fifty-thousand cells per sample were analyzed for quantification of the fluorescence signal. (**C**) Internalization of TB4 peptide in the presence of cellular uptake inhibitors. RAW264.7 cells were treated with various inhibitors, followed by treatment with FAM-TB4 peptide. The cells were treated with FAM-TB4 peptide at 4°C for 2 hours for cold inhibition. The fluorescent signal from the internalized FAM-TB4 peptide was quantified by flow cytometry where 50,000 cells per sample were analysed for quantification. (**D**) Fluorescent microscopy images of RAW264.7 cells treated with FAM-TB4 in the presence of Nocodazole, MβCD, or cold temperature treatment. The cells were imaged using a fluorescence microscope at 63×. Scale bar, 50 μm. Image represents 15 different fields captured from cells treated with inhibitors and TB4. (**E** and **F**) Flow cytometry analysis of RAW264.7 cells treated with increasing concentrations of MβCD (**E**) and Nocodazole (**F**), followed by treatment with FAM-TB4 peptide. The data are presented as the mean ± SEM from at least two independent experiments (n.s, P > 0.05;*, P< 0.05; **, P< 0.01; ***, P < 0.001; ****, P < 0.0001).

https://doi.org/10.2147/JIR.S526902

peptides and analysed the release of LDH in the culture supernatants. None of the peptides induced any cytotoxicity in the treated macrophages (Figure 3C). Next, we examined the efficiency of TcpB and TIRAP-derived peptides to suppress the LPS-induced production of pro-inflammatory cytokines in macrophages. The peptide-treated macrophages were induced with LPS, followed by analysing the production of TNF-α and IL-6 by qRT-PCR and ELISA. We found that TB4-BBL peptides could suppress the induction of pro-inflammatory cytokines as efficiently as the control peptides (Figure 3D, Appendix Figure S2C-E). Since the TB4-BBL2 peptide was identified as the shortest peptide exhibiting maximum efficacy in suppressing pro-inflammatory cytokines secretion, along with minimal cytotoxicity and efficient cell-permeability, this peptide was selected for further experiments.

Macrophages treated with increasing concentrations of TB4-BBL2 showed a dose-dependent suppression of TNF-α and IL-6, confirming its anti-inflammatory property (Figure 3E–H, Appendix Figure S2F and G). To evaluate the efficacy of TB4-BBL2 in modulating TLR-driven inflammatory responses, RAW264.7 cells were pre-treated with increasing concentrations of TB4-BBL2, followed by stimulation with TLR ligands- Pam3CSK4 (TLR2 agonist), ODN (TLR9 agonist), and Poly I:C (TLR3 agonist). The levels of TNF-α in the supernatant were quantified by ELISA. TB4-BBL2 treatment resulted in a dose-dependent suppression of TNF-α production induced by TLR2/9 agonists (Figure 3I). Next, we examined the efficacy of TB4-BBL2 to suppress LPS-induced NF-κB activation, which drives the expression of pro-inflammatory cytokines in macrophages. RAW264.7 cells were transfected with the luciferase reporter plasmids, followed by treatment with various concentrations of TB4-BBL2 peptide. The luciferase activity, driven by NF-κB activation, was quantified after stimulating the cells with LPS. The TB4-BBL2 peptide could efficiently suppress the activation of NF-κB in a dose-dependent manner (Figure 3J).

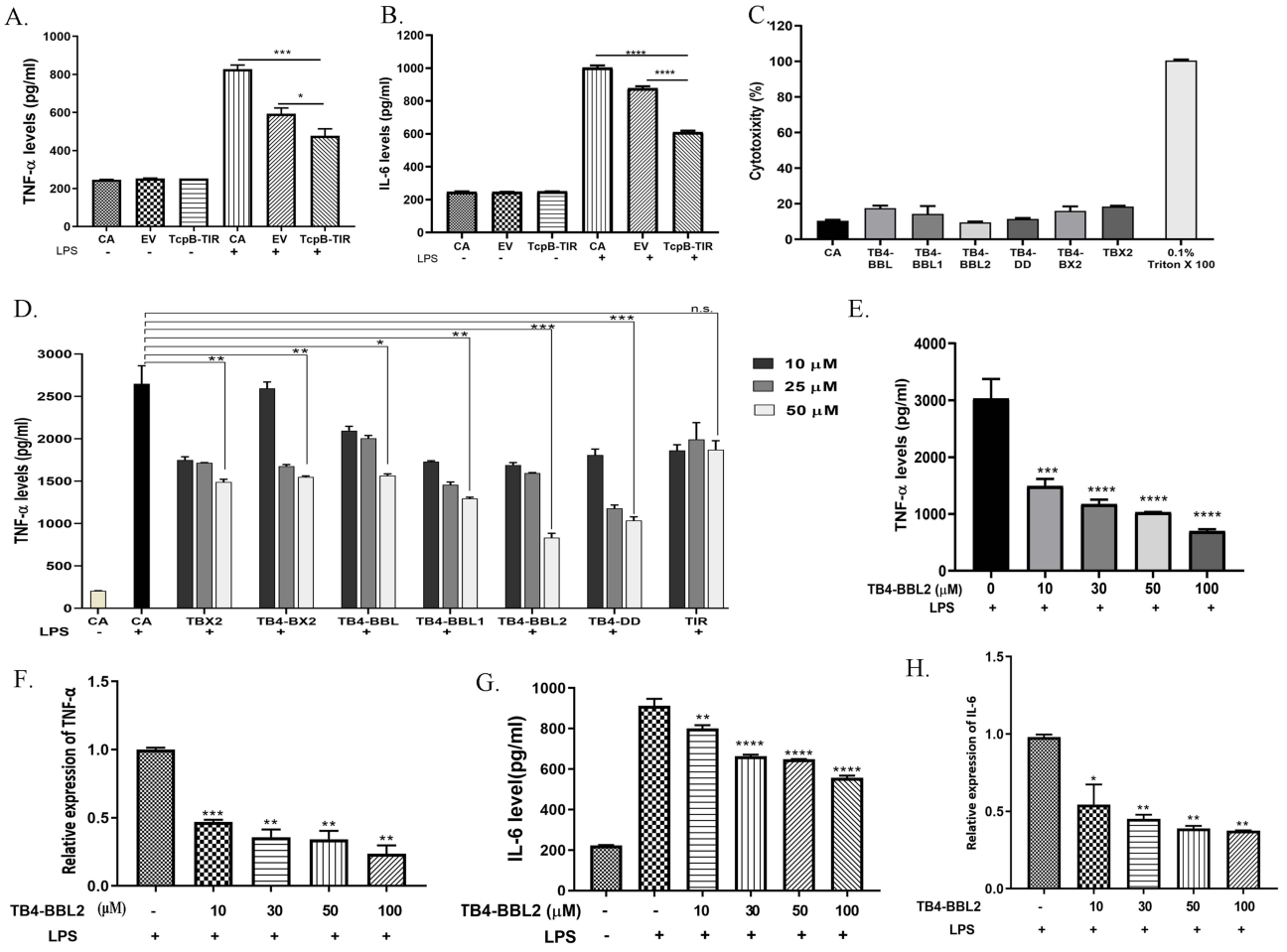

Figure 3 Continued.

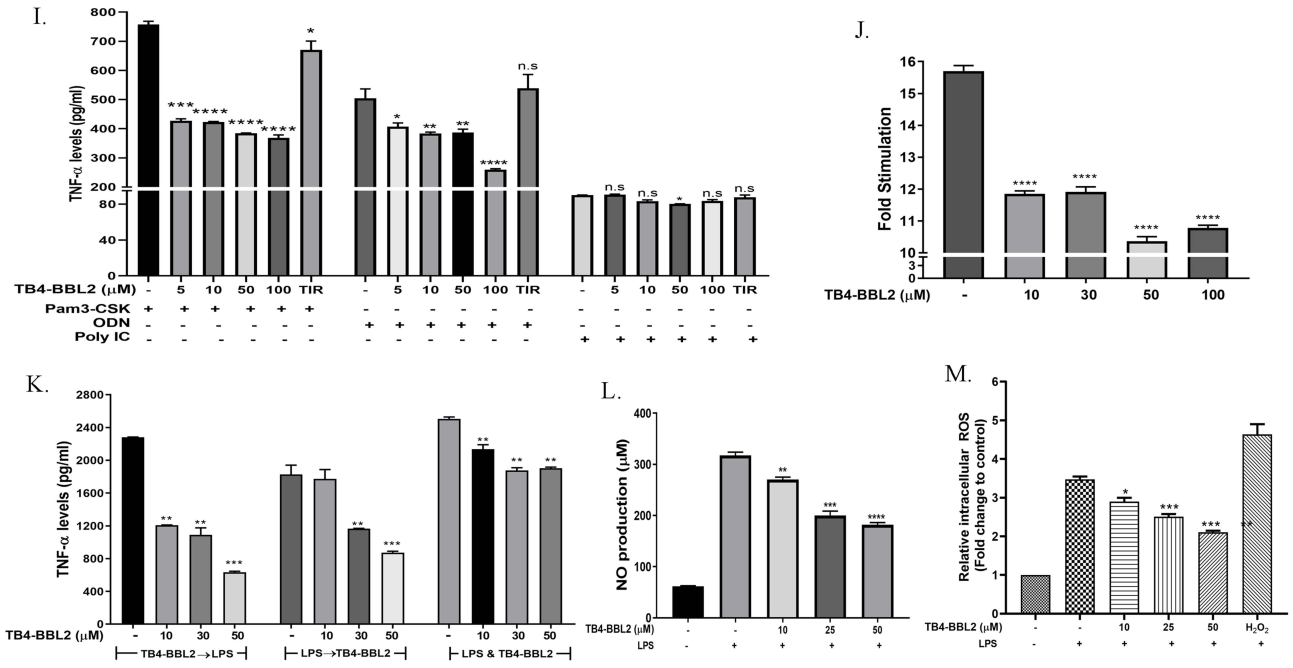

Figure 3 Generation of cell permeable, anti-inflammatory peptide from TcpB. (**A** and **B**) The TIR domain of TcpB suppresses LPS-induced pro-inflammatory cytokines in macrophages. RAW264.7 cells were transfected with eukaryotic expression plasmid harboring the TIR domain of TcpB, followed by inducing the cells with LPS. The levels of secreted TNF-α (**A**) and IL-6 (**B**) were quantified by ELISA. (**C**) LDH assay to determine the cytotoxicity of TcpB or TIRAP-derived peptides. Immortalised BMDM cells were treated with 100 μM of indicated peptides for 5 hours, followed by quantifying the LDH released into the culture supernatants. (**D**) The chimeric peptides from TcpB or TIRAP suppress LPS-induced production of TNF-α. RAW264.7 cells were treated with the indicated peptides, followed by the induction of pro-inflammatory cytokines by LPS. The levels of TNF-α in the LPS-induced cells were quantified by ELISA. (**E**) ELISA showing the levels of LPS-induced TNF- α in RAW264.7 cells treated with increasing concentrations of TB4-BBL2. (**F**) qPCR data showing the LPS-induced TNF- α levels in RAW264.7 cells treated with increasing concentrations of TB4-BBL2. (G&H) ELISA (**G**) and q-RT-PCR (**H**) data showing the levels of LPS-induced IL-6 in RAW264.7 cells treated with increasing concentrations of TB4-BBL2. (**I**) TB4-BBL2 suppresses TLR2/4/9-mediated production of TNF-α. RAW264.7 cells were treated with increasing concentrations of TB4-BBL2, followed by the induction of pro-inflammatory cytokines by various TLR ligands; Pam3-CSK-TLR2, ODN-TLR9, Poly I:C-TLR3. The levels of TNF-α in the supernatant were quantified by ELISA. (**J**) Attenuation of LPS-induced NF-κB activation by TB4-BBL2 peptide in macrophages. RAW264.7 cells were transfected with luciferase reporter plasmids and treated with increasing concentrations of TB4-BBL2 peptide. Twenty-four hours post-transfection, cells were induced with LPS, followed by quantification of luciferase activity. The data are represented as relative luminescence units of NF-κB activation in the uninduced vs LPS-induced cells. (**K**) Efficacy of TB4-BBL2 peptide to attenuate TNF-α, which is induced prior, after, or simultaneous treatment with LPS. RAW264.7 cells were first treated with TB4-BBL2 peptide, followed by LPS induction or first induced with LPS, followed by peptide treatment or treated with peptide and LPS together. The levels of secreted TNF-α in the culture supernatants were quantified by ELISA. (**L**) TB4-BBL2 peptide attenuates LPS-induced production of NO in macrophages. RAW264.7 cells were treated with increasing concentrations of TB4-BBL2, followed by induction with LPS and quantification of NO levels by Griess assay. (**M**) Attenuation of LPS-induced ROS by TB4-BBL2 peptide. RAW264.7 cells were treated with increasing concentrations of TB4-BBL2 peptide, followed by inducing cells with LPS. Subsequently, the cells were treated with H2DCFDA for 30 minutes, and the formation of DCF was measured using a multi-mode reader with excitation at 492 nm and emission at 517 nm. The data are presented as the mean ± SEM from at least three independent experiments (n.s, P > 0.05;*, P< 0.05; **, P< 0.01; ***, P < 0.001; ****, P < 0.0001).
Abbreviations: EV, Empty vector; CA, Cell alone.

Next, we analysed the TB4-BBL2-mediated suppression of pro-inflammatory cytokines in macrophages upon pre- or post-LPS treatment. The TB4-BBL2-treated macrophages were induced with LPS, or LPS-induced macrophages were treated with TB4-BBL2. The TB4-BBL2 peptide could efficiently suppress the production of TNF-α in both conditions (Figure 3K). Simultaneous treatment of macrophages with LPS and TB4-BBL2 showed decreased efficiency compared to the conditions mentioned above (Figure 3K). In addition to pro-inflammatory cytokines, LPS induces the production of reactive oxygen species (ROS) and nitric oxide (NO) in endotoxemia. Therefore, we sought to examine the levels of LPS-induced ROS and NO in TB4-BBL2-treated macrophages. RAW264.7 cells were stimulated with LPS, followed by treating the cells with the TB4-BBL2 peptide and quantifying ROS and NO. The TB4-BBL2 peptide could efficiently suppress the LPS-induced generation of ROS and NO in the macrophages (Figure 3L and M). Our experimental data suggest that macrophages uptake the TB4-BBL2, and the internalized peptide could efficiently suppress LPS-induced activation of NF-κB, production of pro-inflammatory cytokines, ROS, and NO.

https://doi.org/10.2147/JIR.S526902

TB4-BBL2 Targets TIRAP and MYD88 to Negatively Regulate LPS Signalling

Since the TB4-BBL2 peptide interferes with LPS signalling, we wished to examine its mechanism of action. TcpB has been reported to interact with TLR2/4 adaptor proteins, TIRAP, and MYD88.[10,12] TcpB-mediated ubiquitination and degradation of TIRAP have also been reported[12,14] Therefore, we examined whether the TB4-BBL2 peptide interacts with TIRAP or MYD88 by co-immunoprecipitation. FLAG-EV was used as an experimental negative control because it does not produce any functional protein that could interact with the peptides, thus serving as a baseline for background fluorescence. We used an unrelated host protein, USP8, and TB4 or TAT peptide as controls to ensure the specificity of TB4-BBL2 interaction. HEK293T cells over-expressing FLAG-EV/TIRAP/MYD88/USP8 were lysed, followed by incubating the lysates with FAM-labelled TB4-BBL2/TB4/TAT peptide. Subsequently, FLAG-TIRAP/MYD88/USP8 was immunoprecipitated using the anti-FLAG antibody, and co-immunoprecipitation of FAM-labeled peptide was detected by measuring the fluorescence. We observed enhanced fluorescence in the co-immunoprecipitate of TIRAP or MYD88 with TB4-BBL2 peptide compared to the controls (Figure 4A). Minimal fluorescence levels were detected in the co-immunoprecipitation of TIRAP/MYD88 with TB4 and TAT peptide, indicating the specificity of TIRAP and MYD88 interaction with the TB4-BBL2 peptide. Additionally, minimal fluorescence was observed in the co-immunoprecipitation assays involving FLAG-EV or FLAG-USP8 with TB4-BBL2, further highlighting the strong and specific interaction between the TB4-BBL2 peptide and TIRAP/MYD88. To reconfirm the interaction further, we examined the binding affinity between FAM-TB4-BBL2 and purified recombinant MBP-TIRAP protein or MBP alone using a microscale thermophoresis assay. A Kd value of 99.6 nM ± 64.0 nM was observed between FAM-TB4-BBL2 and MBP-TIRAP compared to the MBP alone, indicating a positive interaction (Figure 4B). Collectively, our experimental data suggest that TB4-BBL2 specifically interacts with the TLR2/4 adaptor proteins TIRAP and MYD88.

Given that TB4-BBL2 interacts with TIRAP and MYD88, we sought to examine whether TB4-BBL2 induces the degradation of its binding partners. RAW264.7 cells were treated with TB4-BBL2 peptide, followed by analysing the endogenous levels of TIRAP and MYD88. We observed an enhanced degradation of endogenous TIRAP and MYD88 with TB4-BBL2 treatment (Figure 4C and D). We also treated macrophages with the TIR peptide alone, which is impermeable to the cells. The TIR peptide did not induce degradation of TIRAP or MYD88, suggesting that cell penetration of the peptide is essential for promoting their degradation (Figure 4C). To further validate these findings, the cells were treated with increasing concentrations of TB4-BBL2 and the levels of TIRAP, and MYD88 were assessed. A similar assay was performed for TLR2 and another adaptor protein TRIF to evaluate the specificity of TB4-BBL2. We observed a concentration-dependent reduction in TIRAP and MYD88 levels with TB4-BBL2 treatment, while TLR2 and TRIF levels remained unchanged (Figure 4D). These results suggest that TB4-BBL2 specifically targets the degradation of the adaptor proteins TIRAP and MYD88, which explains our previous observation that TB4-BBL2 treatment did not affect TLR3-TRIF–induced TNF-α production.

Next, we performed a pulse-chase analysis where RAW264.7 cells were treated with TB4-BBL2 in the presence or absence of cycloheximide that can inhibit the synthesis of fresh proteins. The treated cells were harvested at various time points, followed by immunoblotting to detect the endogenous levels of TIRAP/MYD88/TRIF/TLR2. The cycloheximide-treated cells showed enhanced degradation of TIRAP and MYD88 by TB4-BBL2 compared to untreated cells (Figure 4E and F). The levels of TRIF and TLR2 remained unchanged in both cycloheximide-treated and untreated cells in the presence of TB4-BBL2 (Figure 4E and F). Taken together, our experimental data shows that TB4-BBL2 peptide specifically interacts with and degrades TIRAP and MYD88 to suppress the LPS-induced TLR4 signalling.

TB4-BBL2 Peptide Attenuates LPS-Induced Endotoxemia in Mice

Given that TB4-BBL2 attenuates LPS-induced production of pro-inflammatory cytokines, ROS, and NO in macrophages, we sought to examine its protection in LPS-induced endotoxemia in mice. First, we analysed any potential toxicity induced by TB4-BBL2 and its dosage tolerance in mice. BALB/c mice were treated with different concentrations of TB4-BBL2, followed by assessing various parameters for indication of toxicity. The peptide-treated mice showed no signs of toxicity except with the highest concentration (40 mg/kg) of TB4-BBL2 peptide, where the treated mice showed a slight splenomegaly (Figure 5A–C, Appendix Figure S3A-B).

Next, we examined the effect of TB4-BBL2 on LPS-induced production of pro-inflammatory cytokines in mice. BALB/c mice were treated with increasing concentrations of TB4-BBL2, followed by inducing endotoxemia by

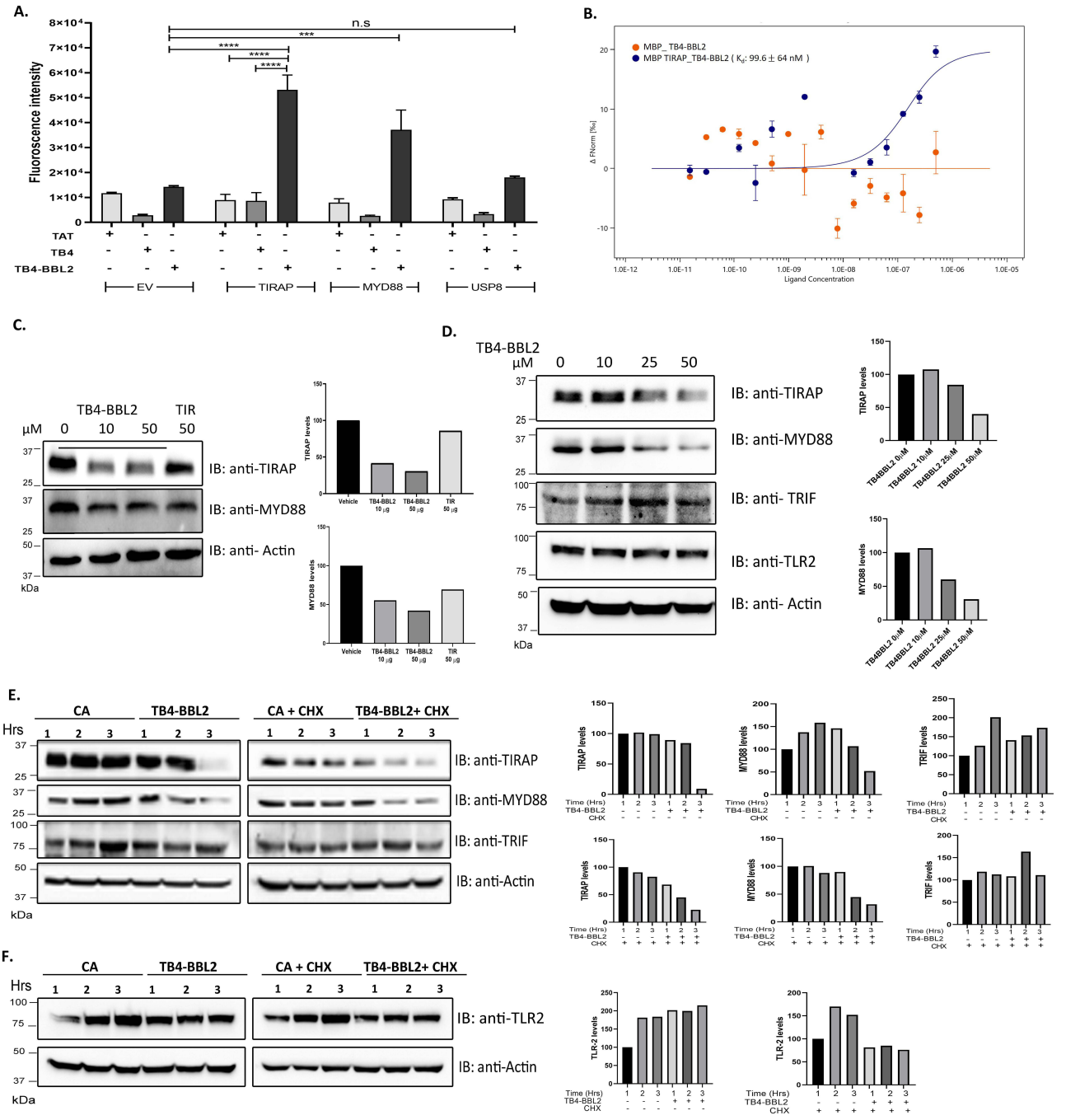

Figure 4 TB4-BBL2 interacts with TIRAP/MYD88 and induces their proteasomal degradation. (**A**) Lysates of HEK293T cells overexpressing Flag-TIRAP/MYD88/USP8/empty vector (EV) were incubated with FAM-labelled TAT/TB4/TB4-BBL2 as indicated in the figure, followed by immunoprecipitation of Flag-tagged proteins. Immunoprecipitation of TIRAP or MYD88 from the lysate incubated with FAM-TB4-BBL2 showed significantly higher fluorescence intensity, indicating co-immunoprecipitation of FAM-TB4-BBL2 due to its interaction with TIRAP or MYD88. (**B**) MST analysis to confirm the interaction between TIRAP and TB4-BBL2. The purified MBP-TIRAP was titrated over a concentration range of 500 nM to 0.01 nM while maintaining a constant concentration of 100 nM for the FAM-TB4-BBL2. The resulting thermophoresis data showed a dissociation constant (Kd) of 99.6± 64.0 nM for MBP-TIRAP and TB4-BBL2 interaction (mean ± SD, *n* = 3 biological independent experiments). (**C**) TB4-BBL2 promotes the degradation of TIRAP and MYD88. RAW264.7 cells were treated with indicated concentrations of TB4-BBL2 or TIR peptide (Table 1). Five hours post-treatment, cells were harvested, followed by immunoblotting and detection of endogenous TIRAP and MYD88. The right side of the panel shows the densitometry of TIRAP and MYD88 bands. (**D**) TB4-BBL2 does not alter the levels of TRIF and TLR2. RAW264.7 cells were treated with indicated concentrations of TB4-BBL2. Five hours post-treatment, cells were harvested, followed by immunoblotting and detection of endogenous proteins, TIRAP, MYD88, TRIF and TLR2. The right side of the panel shows the densitometry of TIRAP and MYD88 bands. (**E** and **F**) Pulse-chase analysis using cycloheximide. RAW264.7 cells were treated with TB4-BBL2 for three hours, followed by treatment with cycloheximide. Subsequently, the cells were harvested at the indicated time points and subjected to immunoblotting. The levels of endogenous TIRAP, MYD88, TRIF and TLR2 were detected in TB4-BBL2 treated cells with increasing time points in the presence or absence of cycloheximide. The right side of the panels shows the densitometry of the TIRAP, MYD88, TRIF and TLR2 bands. Beta actin served as a loading control for all the immunoblots. The immunoblots are representative of three independent experiments. The data are presented as the mean ± SEM from at least three independent experiments (n.s, $P > 0.05$; **, $P < 0.001$; ****, $P < 0.0001$).

Abbreviation: CHX, cycloheximide.

https://doi.org/10.2147/JIR.S526902

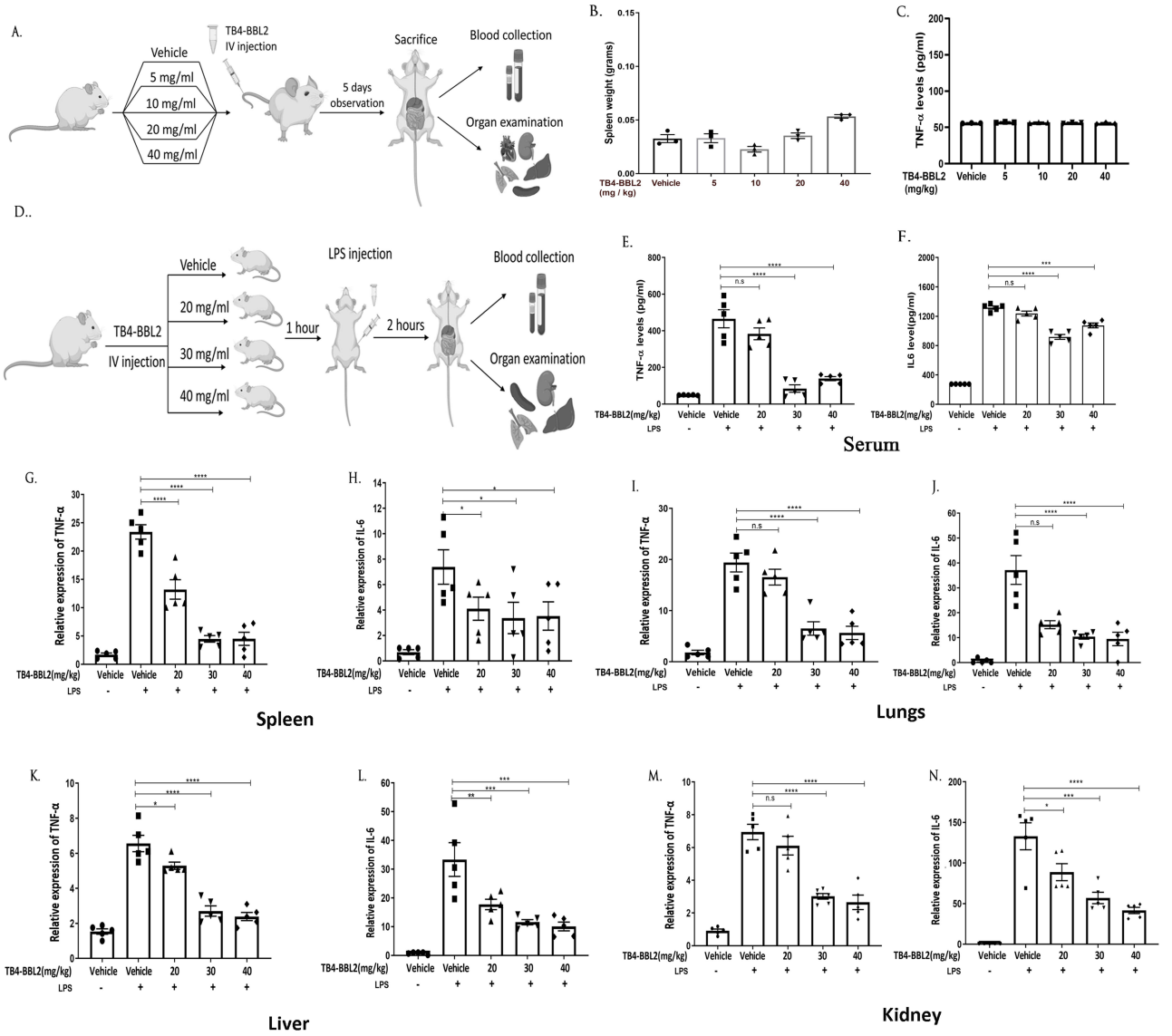

Figure 5 TB4-BBL2 suppresses production of LPS-induced pro-inflammatory cytokines in mice. (**A**) Pictographic representation of study design to analyze the toxicity of TB4-BBL2 peptide in mice. (**B** and **C**) Mice were treated with indicated concentrations of TB4-BBL2 peptide, and the toxicity parameters were evaluated for 5 days, followed by sacrifice of mice and necropsy. The spleen weight of peptide-treated mice was determined (B), and TNF-α level in the serum (**C**) was quantified using ELISA. (**D**) Pictographic representation of the experimental design for evaluating the efficacy of TB4-BBL2 peptide in the mice model of endotoxemia. (**E**–**N**) TB4-BBL2 peptide attenuates LPS-induced production of pro-inflammatory cytokines in mice. Mice were treated with indicated doses of TB4-BBL2 peptide for 1 hour, followed by administration of LPS. Mice were sacrificed 2 hours post-LPS treatment, and the levels of TNF-α (**E**) and IL-6 (**F**) in the serum were quantified by ELISA and mRNA expression levels of TNF-α and IL-6 in the spleen (**G** and **H**), lungs (**I** and **J**), liver, (**K** and **L**) and kidney (**M** and **N**) were estimated by q-RT-PCR. The data are presented as the mean ± SEM of 3 mice per group (n.s, P > 0.05; *, P< 0.05; **, P< 0.01; ***, P < 0.001; ****, P < 0.0001).

administering LPS (Figure 5D). We found a dose-dependent suppression of pro-inflammatory cytokines in the TB4-BBL2 treated mice in the serum, lungs, spleen, liver, and kidneys (Figure 5E–N). Since 30 mg/kg of TB4-BBL2 peptide showed optimal protection, we selected this concentration for further experiments.

Next, we analysed the efficacy of TB4-BBL2 peptide in pre- or -simultaneous induction of endotoxemia by LPS treatment (Figure 6A). Mice treated with LPS, followed by administration of TB4-BBL2 resulted in efficient suppression of pro-inflammatory cytokines (Figure 6B–K). Simultaneous treatment of mice with LPS and TB4-BBL2 peptide also showed protection but not to the extent of the experimental conditions described above (Figure 6B–K).

To evaluate the protective effects of the TB4-BBL2 peptide in endotoxemia, tissue sections from the spleen, lungs, liver, and kidney of control or LPS-treated mice, either untreated or treated with TB4-BBL2, were examined using H&E staining.

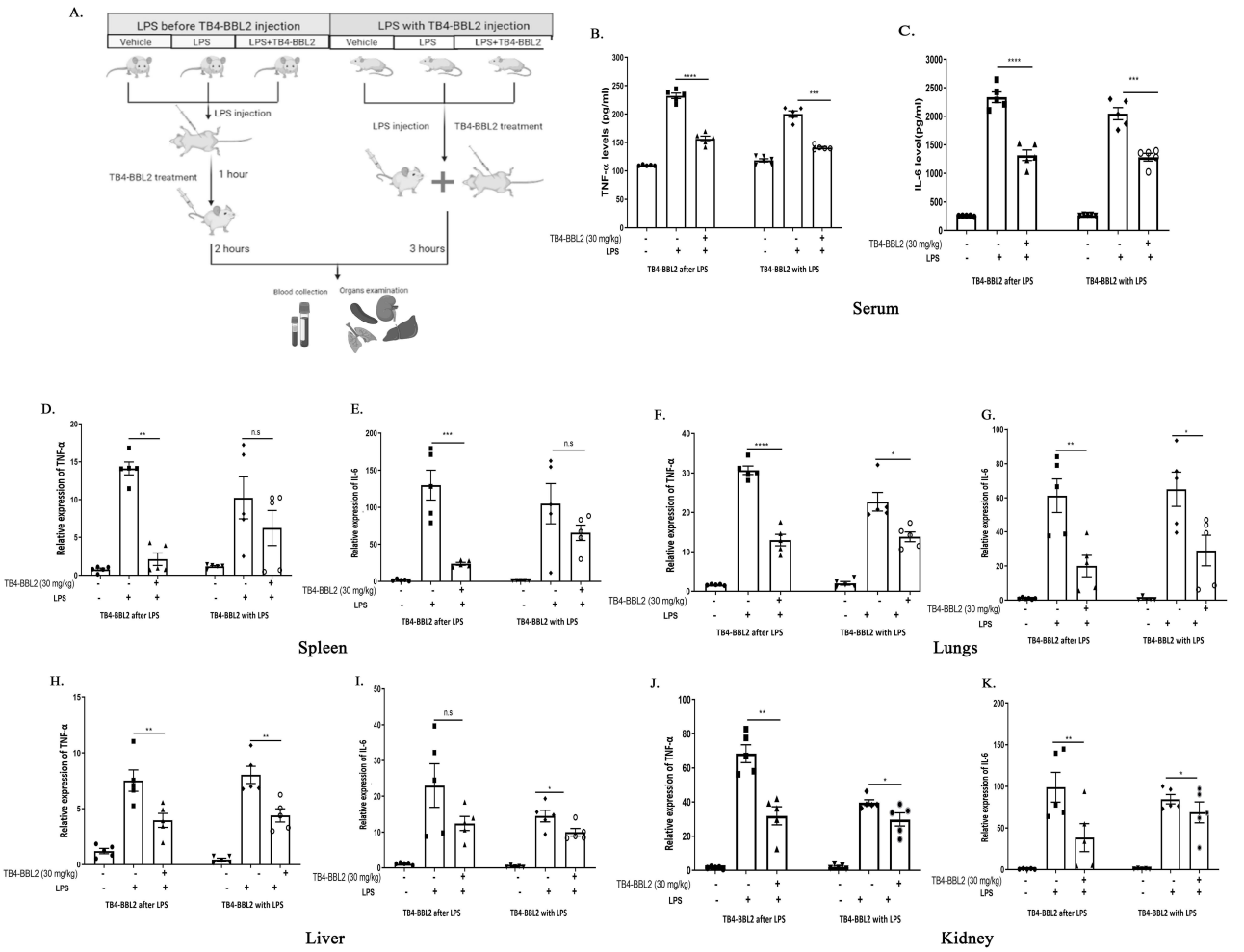

Figure 6 The effect of TB4-BBL2 after LPS treatment or simultaneous treatment of mice with TB4-BBL2 and LPS. (**A**) Pictographic representation of the experimental design. (**B**–**K**) The levels of TNF-α and IL-6 in the serum (**B** and **C**), spleen (**D** and **E**), lungs (**F** and **G**), liver (**H** and **I**), and kidneys (**J** and **K**) of mice in two experimental conditions such as TB4-BBL2 treatment after LPS administration or simultaneous delivery of TB4-BBL2 and LPS. The data are presented as the mean ± SEM of 5 mice per group (n.s, P > 0.05; *, P< 0.05; **, P< 0.01; ***, P < 0.001; ****, P < 0.0001).

Endotoxemia induced by LPS administration resulted in significant tissue injury, characterized by extensive inflammatory cell infiltration and the presence of necrotic foci. These pathological features were markedly reduced in the TB4-BBL2-treated group, highlighting its potential to mitigate tissue damage associated with endotoxemia (Appendix Figure S3C and D). Taken together, our experimental data indicate that TB4-BBL2 can efficiently suppress the production of pro-inflammatory cytokines in the mice model of endotoxemia without showing any signs of toxicity.

Conjugation of Gentamicin with TcpB-Derived Peptide Enhances Its Intracellular Availability

The antibiotic, gentamicin, displays a wide spectrum of bactericidal activity against several Gram-negative bacteria. However, it is semi-permeable to cells, limiting its application for treating infections caused by intracellular bacterial pathogens. In this study, we analyzed whether the conjugation of gentamicin with TcpB-derived peptides can improve its cell permeability. Gentamicin was conjugated to the added cysteine residue of TB4 using the cross-linker SMCC, and the efficiency of the conjugation process was evaluated using Ellman's reagent, which detects free thiol groups of unconjugated peptides in the reaction mixture (Figure 7A). We observed an increasing concentration gradient of free thiol groups in unconjugated cTB4, whereas the negligible detection of thiol groups in cTB4-G indicated an efficient conjugation of cTB4 with gentamicin through SMCC (Figure 7B). Next, we evaluated the antimicrobial properties of cTB4-conjugated gentamicin against *B. neotomae* and *S. typhimurium*. We did not observe any difference in antibacterial

https://doi.org/10.2147/JIR.S526902

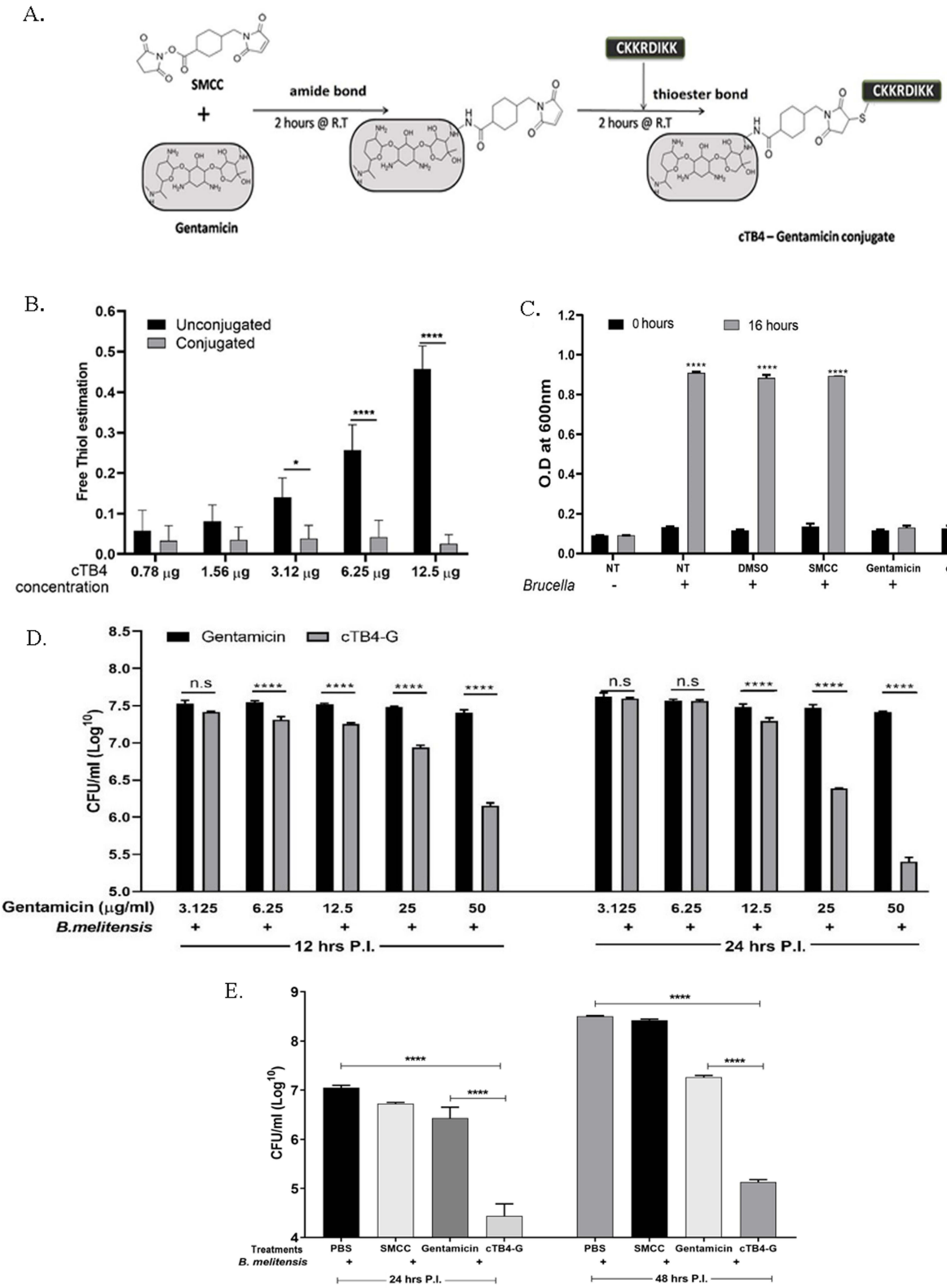

Figure 7 Conjugation of gentamicin with cTB4 enhances its cellular availability (**A**) Pictographic representation of conjugation of gentamicin with cTB4 using SMCC as the cross-linker. (**B**) Evaluating the efficiency of conjugation using Ellman's reagent. The conjugated or unconjugated cTB4 was incubated with DNTB reagent, followed by measuring the OD at 412 nm. (**C**) Conjugation of gentamicin to cTB4 did not affect its antimicrobial activity. *B. neotomae* cultures were incubated with gentamicin alone or cTB4-gentamicin, followed by measuring OD 600 nm after sixteen hours (**D**) Antibacterial activity of increasing concentrations of cTB4-gentamicin against the intracellular localised *B. melitensis*. *B. melitensis*-infected macrophages were treated with indicated concentrations of cTB4-gentamicin, followed by the enumeration of CFU at 12 and 24 hours post-infection. (**E**) Antibacterial activity of cTB4-gentamicin against the intracellular localised *B. melitensis* at various treatment times. *B. melitensis*-infected macrophages were treated with cTB4-gentamicin conjugate for the indicated time points, followed by enumerating CFU. The data are presented as the mean ± SEM from at least two independent experiments (n.s, $P > 0.05$; *, $P < 0.05$; ****, $P < 0.0001$).

properties between gentamicin alone and gentamicin-TB4 conjugate, suggesting that TB4 conjugation did not impair the activity of gentamicin (Figure 7C, Appendix Figure 4A). No significant growth inhibition was observed when the bacterial cultures were treated with DMSO or SMCC alone. We further analyzed the concentration of gentamicin-cTB4 required for optimal antibacterial activity by performing a gentamicin titration assay. Macrophages were infected with the highly infectious intracellular bacterial pathogen, *B. melitensis* and subsequently treated with various concentrations of gentamicin-TB4 conjugate or gentamicin alone. We found that 50 μg/mL of cTB4-G exhibited the maximum antibacterial potency as compared to gentamicin alone at both 12- and 24 hours post-treatment (Figure 7D). Furthermore, we observed a significant reduction of *Salmonella/B. melitensis* load in the infected macrophages with increasing treatment time (Figure 7E, Appendix Figure S4B-D).

Treatment of *B. melitensis*-Infected Mice with cTB4-BBL2-Gentamicin Results in Enhanced Bacterial Clearance and Suppression of Inflammatory Cytokines

TB4-BBL2 peptide from TcpB protein exhibits excellent cell permeability and anti-inflammatory properties. Therefore, we conjugated gentamicin with cTB4-BBL2 to generate a hybrid drug (cTB4-BBL2-G) with cell permeability and antibacterial and anti-inflammatory properties. To evaluate its efficacy, we treated *Brucella*-infected macrophages with cTB4-BBL2-G, followed by enumerating the CFU and quantifying the levels of TNF-α. We observed enhanced elimination of intracellular *B. melitensis* (Figure 8A and B) as well as suppression of TNF-α in the infected macrophages treated with cTB4-BBL2-G (Figure 8C).

Next, we examined the antibacterial and anti-inflammatory efficacy of cTB4-BBL2-Gentamicin in the mice model of brucellosis. Ten days after infection with *B. melitensis*, BALB/c mice were treated with cTB4-BBL2-gentamicin or control treatments, including PBS, gentamicin alone, or cTB4-Gentamicin, for three consecutive days. On day 14 post-infection, the mice were sacrificed, and the bacterial load in the spleen was quantified by CFU enumeration (Figure 8D). We observed a significant reduction in *B. melitensis* load in the spleens of mice treated with c-TB4-Gentamicin or cTB4-BBL2-Gentamicin compared to those treated with gentamicin alone (Figure 8E). Further, we analysed the levels of TNF-α in the serum of mice in all experimental groups. Mice treated with cTB4-BBL2-Gentamicin exhibited significantly lower serum TNF-α levels compared to the other treatment groups (Figure 8F). Additionally, spleen, lungs, liver, and kidneys from each treatment group were examined for the expression of pro-inflammatory cytokine genes. In all analyzed organs, the cTB4-BBL2-Gentamicin treatment group showed a marked reduction in the expression levels of both TNF-α and IL-6 compared to the other groups (Figure 8G–J).

Discussion

Toll-like receptors play an indispensable role in the innate immunity of mammals by recognizing invaded microbial pathogens and inducing various protective immune responses, including adaptive immunity.[34,35] There are twelve reported TLRs in mice, and ten in humans localized both on the cell surface and intracellular endolysosomal compartments of various cell types such as monocytes, macrophages, dendritic cells, neutrophils, B cells, T cells, and fibroblasts.[36,37] The activation of TLRs by PAMPs leads to the recruitment of the TIR domain-containing adaptor proteins, and this molecular assembly activates various downstream proteins. The TLR signalling results in the production of pro-inflammatory cytokines, chemokines and many anti-microbial compounds such as nitrogen and oxygen free radicals and anti-microbial peptides. Even though TLRs play an essential role in defence against invaded microbial pathogens, their aberrant activation results in the pathogenesis of various inflammatory and infectious diseases. Therefore, the overactivation of TLR signalling is prevented by expressing multiple negative regulators of TLRs such as IRAK-M, SOCS1, Triad3A, and Toll-interacting protein.[38–41] Some of these intracellular regulators are inherently present to regulate TLR activation at a physiological level, while others are upregulated through TLR signalling during infections.[42] Since TLR triggers anti-microbial responses, many pathogenic microorganisms encode virulence factors that negatively regulate the TLR signalling. Many bacterial pathogens harbour proteases, acetyltransferases, kinases, deubiquitinases, or TIR-domain-containing proteins to subvert the TLR signalling.[8] The food-borne pathogen *Salmonella enteritidis* secretes the TIR domain-containing protein, TlpA, to inhibit the TLR/IL1 induced NF-κB activation.[43]

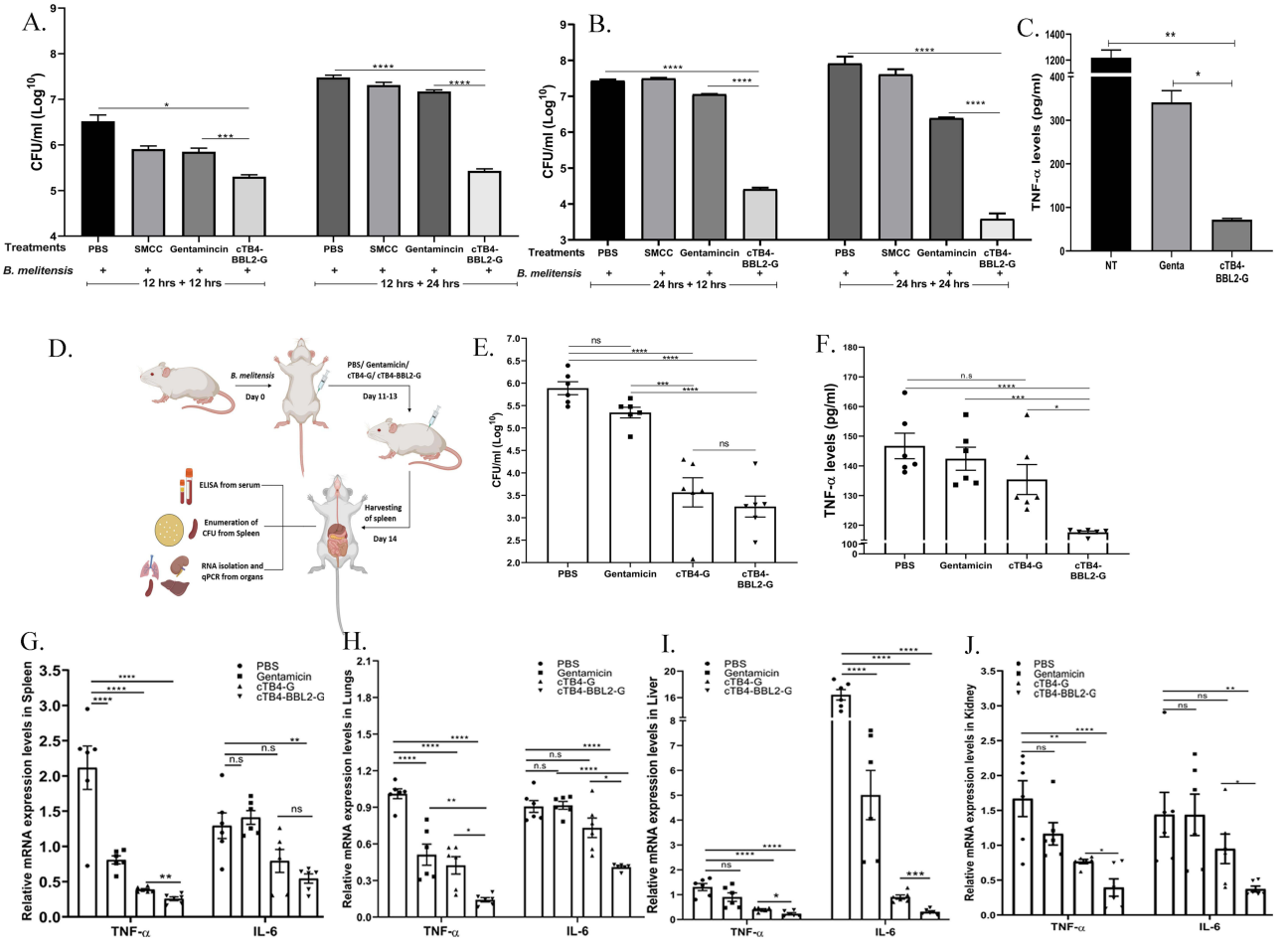

Figure 8 Conjugating gentamicin with cTB4-BBL2 enhances cell permeability and imparts anti-inflammatory properties. (**A** and **B**) Macrophages were infected with *B. melitensis* for 12 hours (**A**) or 24 hours (**B**), followed by treatment with cTB4-BBL2-Gentamicin. The CFU was enumerated 12 or 24 hours post-treatment. (**C**) Treatment of *B. melitensis* infected macrophages with cTB4-BBL2-Gentamicin for 48 hours, followed by collection of supernatant and quantification of TNF-α by ELISA. (**D**) Schematic diagram showing the methodology used for examining the effect of cTB4-BBL2-Gentamicin treatment in *B. melitensis* infected mice. (**E**) Scatter plot showing the splenic load of *B. melitensis* in the mice treated with cTB4-BBL2-Gentamicin or indicated controls. (**F**) The levels of TNF-α in the serum of mice treated with TB4-BBL2-Gentamicin or indicated controls. (**G**–**J**) mRNA expression levels of TNF-α and IL-6 in the spleen (**G**), lungs (**H**), liver (**I**) and kidney (**J**) of cTB4-BBL2-Gentamicin treated mice or indicated controls by q-RT-PCR. The data are presented as the mean ± SEM of 6 mice per group (n.s, P > 0.05;*, P< 0.05; **, P< 0.01; ***, P < 0.001, ****, P < 0.0001).

Similarly, the uropathogenic *E. coli* CFT073 secretes the TIR domain protein, TcpC to block the MYD88-dependent signalling cascade.[8,44] The intracellular bacterial pathogen, *Brucella* encodes the TIR domain-containing protein, TcpB that interferes with TLR2/4 signalling.[10,13,14]

Dysregulated inflammatory pathways, including TLR signalling, result in many disorders ranging from acute conditions such as multi-organ failure to chronic conditions, including diabetes and cardiovascular diseases.[45] TLR4 is activated by the PAMPS such as LPS and endogenous damage-associated molecular pattern *viz*. High Mobility Group Box Protein 1, Hyaluronan and HSP70.[46,47] The variety of ligands for TLR4, encompassing both pathogen-related and endogenous substances, implies a potential association of this receptor with numerous disorders, including pathogen-associated diseases. The aberrant activation of TLR4 has been implicated in the onset of septicaemia and cardiovascular disorders.[45] Therefore, TLR4 inhibitors represent promising therapeutic approaches to suppress the production of pro-inflammatory cytokines and other inflammatory mediators. The strategies to block the TLR include neutralizing TLR ligands, blocking the binding of ligands to TLRs or inhibitors that interfere with TLR signalling pathways.[48] Many drugs are in the pipeline targeting TLR signaling pathways for infectious diseases caused by pathogens such as hepatitis C, Hepatitis B, anthrax, and influenza.[49]

The microbial proteins that subvert the TLR4 signalling can serve as promising drugs for dampening inflammatory responses. Even though recombinant protein-based therapeutics have been proven effective in treating various clinical indications, they have many drawbacks, including physiochemical instability, immunogenicity, and suboptimal circulation half-life.[50] In recent decades, peptides have emerged as a unique class of therapeutic agents with intrinsic properties and favourable pharmacodynamic profiles. Peptide-based drugs offer many advantages over protein-based therapeutics because of their high specificity, low toxicity, high diversity, and reduced immunogenicity.[51] Furthermore, lower production cost and ease of production on a large scale using chemical synthesis make peptide-based therapeutics as attractive biopharmaceuticals over small molecule counterparts. From 2016 to 2022, there were 22 FDA-approved peptide-based drugs for a spectrum of diseases, such as hyperglycemia and lupus nephritis.[52] Further, several hundreds of peptide-based therapeutics are currently being evaluated in clinical or pre-clinical trials.[53] Hence, therapeutic peptides are promising candidates for developing novel interventions to treat inflammatory disorders.

In this study, we designed and synthesized several peptides from the TcpB protein of *Brucella*, followed by the detailed characterization of these peptides. TcpB is a cell-permeable protein, and this property has been attributed to its PIP binding motif at the N-terminus. Therefore, we designed many peptides from the PIP-binding motif of TcpB and identified the shortest peptide, TB4, that retains the cell-permeable property of TcpB. Furthermore, the TB4 peptide demonstrated excellent cell permeability across various macrophage types. Such intracellular translocation of proteins or peptides typically occurs via diverse mechanisms, including endocytosis.[54] The endocytosis through caveolae, which contain lipid rafts rich in cholesterol and phospholipids, mediates the internalization of various ligands, such as cholera toxin B and albumin.[54] The pharmacological inhibitor of this pathway, MβCD, which depletes cholesterol from lipid rafts, affected the internalization of the TB4 peptide. This implies that TB4 is endocytosed through cholesterol-rich microdomains of the plasma membrane. The arginine and lysine residues in TB4 are essential for internalization as their replacement with alanine affected the cell permeability of TB4. The mutations of basic amino acids to alanine in the PIP-binding motif of TcpB have been reported to affect its property to bind to the phospholipids.[11] Therefore, it can be assumed that the TB4 peptide binds to the phospholipids in the lipid raft to facilitate its internalization through endocytosis. The microtubule polymerization inhibitor, nocodazole, also affected the internalization of the TB4 peptide, suggesting the requirement of intact microtubule for endocytosis of TB4 as reported for uptake of other macromolecules.[55,56] The reduced uptake of TB4 at 4 °C indicates that its internalization does not occur through direct translocation, but instead involves active uptake mechanisms specific to phagocytic cells. The cold inhibition of TB4 internalization further indicates the requirement of ATP, which is in agreement with the fact that endocytosis is an energy-dependent process.[57,58]

The TIR domain is essential for TcpB to interfere with the TIRAP/MYD88 signaling. Overexpression of TIR domain in macrophages suppressed the LPS-induced production of pro-inflammatory cytokines. Previous studies have shown that the intact BB-loop of TcpB is required to inhibit TLR4 signalling.[14] This encouraged us to design peptides from the BB-loop region of TcpB to identify a peptide that mimics the TLR suppression property of TcpB. Since the peptides derived from the TIR domain have no cell permeability, we conjugated them with the TB4 peptide. We evaluated the efficacy of various chimeric peptides and identified the shortest peptide, TB4-BBL2 that exhibited interference with the TIRAP/MYD88 signalling. The TB4-BBL2 peptide could efficiently suppress the NF-κB activation as well as LPS/Pam3-CSK and ODN-induced production of pro-inflammatory cytokines, ROS, and NO in macrophages. The cross-talk between NF-κB, TNF-α, and free radicals is known to play a crucial role in regulating inflammation.[59]

TcpB has been reported to target the adaptor proteins of TLR4 *viz*. TIRAP and MYD88 to interfere with the TLR4 signalling. Therefore, we examined whether the TB4-BBL2 peptide mimics this property of TcpB. The co-immunoprecipitation of TB4-BBL2 with TIRAP and MYD88 suggests that the peptide binds to these adaptor proteins. To confirm the experimental data further, we used the MST technique to analyze the potential interaction between FAM-labelled TB4-BBL2 and recombinant MBP-TIRAP protein. The MST is a biophysical technique to quantitatively assess the interaction between biomolecules.[60,61] The change in fluorescence intensity served as an indicator of the binding event occurring due to the establishment of a thermal gradient induced by infrared light. These variations in fluorescence, resulting from thermophoresis shifts induced by ligand binding, were employed to calculate equilibrium binding constants.[62–64] The MST analysis showed a Kd value of 99.6 ± 64.0 nM between FAM-TB4-BBL2 and MBP-TIRAP compared to MBP alone. This indicates a positive interaction between FAM-TB4-BBL2 and MBP-TIRAP. The lower Kd value between the target TB4-BBL2 and ligand MBP-TIRAP indicates a positive interaction. TcpB has been reported to

induce enhanced ubiquitination and degradation of TIRAP to deplete this adaptor protein to enable the negative regulation of TLR4 signalling.[12] Interestingly, we found that the TB4-BBL2 peptide also promotes the targeted degradation of TIRAP and MYD88. However, further studies are needed to elucidate the precise mechanism by which TB4-BBL2 facilitates the degradation of these TLR adaptor proteins.

Toxicity is a major limiting factor that compromises the use of proteins or peptide-based therapeutics. TB4-BBL2 did not induce any toxicity in the cells, as demonstrated by the negligible release of LDH by the peptide-treated cells. Further, we analysed the toxicity and dosage levels of TB4-BBL2 in mice. The mice tolerated peptide concentrations up to 40 mg/kg, with only slight splenomegaly observed at this higher dose of TB4-BBL2. Therefore, a dose of 30 mg/kg was selected to evaluate the efficacy of the TB4-BBL2 peptide in the mouse model of endotoxemia. LPS treatment in mice induces endotoxemia, characterized by elevated levels of pro-inflammatory cytokines and organ injury. We evaluated the effect of TB4-BBL2 under three conditions such as peptide treatment followed by LPS administration, simultaneous delivery of peptide and LPS and peptide treatment after LPS administration. Administration of the peptide, either prior to or following LPS challenge, significantly attenuated pro-inflammatory cytokine production in mice. The significant suppression of pro-inflammatory cytokines by TB4-BBL2 following endotoxemia induction highlights its therapeutic potential for disorders caused by aberrant activation of TLR4. Importantly, the demonstrated in vivo efficacy of TB4-BBL2 peptide underscores its translational potential, especially in acute inflammatory conditions such as sepsis and endotoxemia, where timely modulation of TLR4 signalling is critical. The protective effect of TB4-BBL2, even after inflammation has begun, emphasizes its translational potential as a prophylactic and post-exposure agent.

Treating intracellular infection remains particularly challenging due to the poor cell permeability of conventional antimicrobial agents.[25] Although some antimicrobials exhibit limited cell permeability, their higher doses and prolonged treatment can lead to severe side effects. Furthermore, the rapid emergence of antimicrobial resistance has significantly narrowed the range of effective antibiotics. As novel antibiotic discovery is costly and often yields limited success, improving the properties of existing antibiotics represents a practical and promising strategy.[65] The intracellular niche shields pathogens, such as *Brucella, Mycobacterium*, and *Salmonella* from antimicrobial agents, contributing to their chronic persistence and frequent reinfections. To address the challenge of antibiotic delivery to intracellular pathogens, we explored modifying the aminoglycoside antibiotic gentamicin, which is known for its broad-spectrum activity but limited cellular uptake. Conjugation of gentamicin with the TcpB-derived peptide, TB4, enhanced its cellular uptake without compromising its antibacterial properties. Gentamicin alone exhibited limited efficacy against intracellular bacterial pathogens, however, its conjugation with the TB4 peptide significantly enhanced its ability to eliminate intracellular *Brucella* and *Salmonella*. In addition to reducing the intracellular burden of *B. melitensis* within macrophages, the hybrid drug TB4-BBL2-Gentamicin effectively attenuated the secretion of pro-inflammatory cytokines by the infected macrophages. Furthermore, this hybrid drug demonstrated in vivo efficacy in a murine model of brucellosis by significantly reducing the splenic burden of *B. melitensis* and suppressing the expression of pro-inflammatory cytokines in serum and various organs. These findings suggest that conjugating existing antibiotics with TcpB-derived peptides represents a promising strategy to overcome the poor membrane permeability, thereby restoring the efficacy of antibiotics compromised against intracellular pathogens. The desirable properties of TB4, including its small size, ease of synthesis, solubility, and efficient internalization via endocytosis, highlight its potential for wide applications in drug delivery. Moreover, anti-inflammatory peptides derived from TcpB can confer additional properties to antibiotics, beyond improving cell permeability and antimicrobial activity, thereby further enhancing the therapeutic efficacy of this strategy. In summary, our experimental data suggest that peptides derived from the TcpB protein possess significant translational potential for addressing a range of inflammatory disorders and for improving the pharmacokinetic properties of various therapeutic agents.

Data Sharing Statement

The datasets used and/or analysed during the current study are available from the corresponding author on reasonable request.

Acknowledgments

We thank Ms. Rama Devi for assistance in flow cytometry, Mr. Shashikant Gawai for microscopy, and Dr. Jayant Hole and Mr. Raju at the Small Animal Facility of NIAB for help with mice experiments. We also acknowledge the BSL-3/ABSL-3 facility of UoH-NIAB for providing support with all *B. melitensis*-related experiments.

Author Contributions

GR conceived and designed the study. GR, BRN and BP wrote the paper. BRN and BP performed the experiments and analyzed the experimental data. All authors took part in drafting, revising or critically reviewing the article; gave final approval of the version to be published; have agreed on the journal to which the article has been submitted; and agree to be accountable for all aspects of the work.

Funding

We thank the Department of Science & Technology (DST), Ministry of Science and Technology, Government of India (Grant number: VI-D&P/563/206-17/TDT) for funding. We thank the National Institute of Animal Biotechnology (NIAB) for additional funding and experimental facilities. BRN acknowledges a research fellowship [647/(CSIR-UGC NET DEC. 2018)] from the University Grant Commission (UGC), Government of India. BP acknowledges a research fellowship (DST-INSPIRE IF210464) from Department of Science & Technology (DST), Ministry of Science and Technology, Government of India.

Disclosure

Dr Girish Radhakrishnan reports a patent 556338 licensed to National Institute of Animal Biotechnology and Department of Science and Technology. The authors declare that they have no known competing financial interests or personal relationships that could have appeared to influence the work reported in this paper.

References

1. O'Neill LA, Bowie AG. The family of five: TIR-domain-containing adaptors in toll-like receptor signalling. *Nat Rev Immunol*. 2007;7(5):353–364. doi:10.1038/nri2079
2. Rybka J, Becker CE, O'Neill LA. Inflammasomes in inflammatory disorders: the role of TLRs and their interactions with NLRs. *Int J Mol Sci*. 2007;29(3):239–248.
3. O'Neill LA, Bryant CE, Doyle SL. Therapeutic targeting of Toll-like receptors for infectious and inflammatory diseases and cancer. *Pharmacol Rev*. 2009;61(2):177–197. doi:10.1124/pr.109.001073
4. Piccinini AM, Midwood KS. DAMPening inflammation by modulating TLR signalling. *Mediators Inflam*. 2010;2010:1–21. doi:10.1155/2010/672395
5. Wei J, Zhang Y, Li H, Wang F, Yao S. Toll-like receptor 4: a potential therapeutic target for multiple human diseases. *Biomed Pharmacother*. 2023;166:115338. doi:10.1016/j.biopha.2023.115338
6. Kumar V. Toll-like receptors in sepsis-associated cytokine storm and their endogenous negative regulators as future immunomodulatory targets. *Int Immunopharmacol*. 2020;89(Pt B):107087. doi:10.1016/j.intimp.2020.107087
7. R Salomão BLF, Salomão MC, Santos SS, Azevedo LCP, Brunialti MKC. Sepsis: evolving concepts and challenges. *Braz J Med Biol Res*. 2019;52(4):e8595. doi:10.1590/1414-431x20198595
8. McGuire VA, Arthur JS. Subverting toll-like receptor signaling by bacterial pathogens. *Braz J Med Biol Res*. 2015;6:607.
9. O'Neill LA. Bacteria fight back against Toll-like receptors. *Nat Med*. 2008;14(4):370–372. doi:10.1038/nm0408-370
10. Cirl C, Wieser A, Yadav M, et al. Subversion of Toll-like receptor signaling by a unique family of bacterial toll/interleukin-1 receptor domain-containing proteins. *Nat Med*. 2008;14(4):399–406. doi:10.1038/nm1734
11. Radhakrishnan GK, Splitter GA. Biochemical and functional analysis of TIR domain containing protein from Brucella melitensis. *Biochem Biophys Res Commun*. 2010;397(1):59–63. doi:10.1016/j.bbrc.2010.05.056
12. Sengupta D, Koblansky A, Gaines J, et al. Subversion of innate immune responses by Brucella through the targeted degradation of the TLR signaling adapter, MAL. *J immunol*. 2010;184(2):956–964. doi:10.4049/jimmunol.0902008
13. Salcedo SP, Marchesini MI, Lelouard H, et al. Brucella control of dendritic cell maturation is dependent on the TIR-containing protein Btp1. *PLoS Pathogens*. 2008;4(2):e21. doi:10.1371/journal.ppat.0040021
14. Radhakrishnan GK, Yu Q, Harms JS, Splitter GA. Brucella TIR domain-containing protein mimics properties of the toll-like receptor adaptor protein TIRAP. *J Biol Chem*. 2009;284(15):9892–9898. doi:10.1074/jbc.M805458200
15. Li W, Ke Y, Wang Y, et al. Brucella TIR-like protein TcpB/Btp1 specifically targets the host adaptor protein MAL/TIRAP to promote infection. *Biochem Biophys Res Commun*. 2016;477(3):509–514. doi:10.1016/j.bbrc.2016.06.064
16. Jakka P, Bhargavi B, Namani S, Murugan S, Splitter G, Radhakrishnan G. Cytoplasmic linker protein CLIP170 negatively regulates TLR4 signaling by targeting the TLR adaptor protein TIRAP. *J Immunol*. 2018;200(2):704–714. doi:10.4049/jimmunol.1601559
17. Brandenburg K, Andrä J, Garidel P, Gutsmann T. Peptide-based treatment of sepsis. *Appl Microbiol Biotechnol*. 2011;90(3):799–808. doi:10.1007/s00253-011-3185-7
18. Khalily MP, Soydan M. Peptide-based diagnostic and therapeutic agents: where we are and where we are heading? *Chem Biol Drug Des*. 2023;101(3):772–793. doi:10.1111/cbdd.14180
19. Erak M, Bellmann-Sickert K, Els-Heindl S, Beck-Sickinger AG. Peptide chemistry toolbox - transforming natural peptides into peptide therapeutics. *Bioorg Med Chem*. 2018;26(10):2759–2765. doi:10.1016/j.bmc.2018.01.012
20. Wang L, Wang N, Zhang W, et al. Therapeutic peptides: current applications and future directions. *Signal Transduct Target Ther*. 2022;7(1):48. doi:10.1038/s41392-022-00904-4
21. Kardani K, Milani A, HS S, Bolhassani A. Cell penetrating peptides: the potent multi-cargo intracellular carriers. *Signal Transduct Target Ther*. 2019;16(11):1227–1258.

22. Hymel HC, Rahnama A. How cargo identity alters the uptake of cell-penetrating peptide (CPP)/Cargo Complexes: a study on the effect of net cargo charge and length. *Cells*. 2022;11(7). doi:10.3390/cells11071195
23. Lau JL, Dunn MK. Therapeutic peptides: historical perspectives, current development trends, and future directions. *Cells*. 2018;26(10):2700–2707.
24. Zeiders SM, Chmielewski J. Antibiotic–cell-penetrating peptide conjugates targeting challenging drug-resistant and intracellular pathogenic bacteria. *Chem Biol Drug Des*. 2021;98(5):762–778. doi:10.1111/cbdd.13930
25. Lehar SM, Pillow T, Xu M, et al. Novel antibody-antibiotic conjugate eliminates intracellular S. aureus. *Nature*. 2015;527(7578):323–328. doi:10.1038/nature16057
26. Blair JM, Webber MA, Baylay AJ, Ogbolu DO, Piddock LJ. Molecular mechanisms of antibiotic resistance. *Nat Rev Microbiol*. 2015;13(1):42–51. doi:10.1038/nrmicro3380
27. Munita JM, Arias CA. Mechanisms of antibiotic resistance. *Microbiol Spectrum*. 2016;4(2). doi:10.1128/microbiolspec.VMBF-0016-2015
28. Valkov E, Stamp A, Dimaio F, et al. Crystal structure of Toll-like receptor adaptor MAL/TIRAP reveals the molecular basis for signal transduction and disease protection. *Proc Natl Acad Sci USA*. 2011;108(36):14879–14884. doi:10.1073/pnas.1104780108
29. Alaidarous M, Ve T, Casey LW, et al. Mechanism of bacterial interference with TLR4 signaling by Brucella toll/interleukin-1 receptor domain-containing protein TcpB. *J Biol Chem*. 2014;289(2):654–668. doi:10.1074/jbc.M113.523274
30. Broz P, von Moltke J, Jones JW, Vance RE, Monack DM. Differential requirement for Caspase-1 autoproteolysis in pathogen-induced cell death and cytokine processing. *Cell Host Microbe*. 2010;8(6):471–483. doi:10.1016/j.chom.2010.11.007
31. Murugan S, Nandi BR, Mazumdar V, et al. Outer membrane protein 25 of Brucella suppresses TLR-mediated expression of proinflammatory cytokines through degradation of TLRs and adaptor proteins. *J Biol Chem*. 2023;299(11):105309. doi:10.1016/j.jbc.2023.105309
32. Low W, Mortlock A, Petrovska L, Dottorini T, Dougan G, Crisanti A. Functional cell permeable motifs within medically relevant proteins. *J Biotechnol*. 2007;129(3):555–564. doi:10.1016/j.jbiotec.2007.01.019
33. Radhakrishnan GK, Harms JS, Splitter GA. Modulation of microtubule dynamics by a TIR domain protein from the intracellular pathogen Brucella melitensis. *Biochem J*. 2011;439(1):79–83. doi:10.1042/BJ20110577
34. Lapaque N, Takeuchi O, Corrales F, et al. Differential inductions of TNF-alpha and IGTP, IIGP by structurally diverse classic and non-classic lipopolysaccharides. *Cell Microbiol*. 2006;8(3):401–413. doi:10.1111/j.1462-5822.2005.00629.x
35. Akira S, Uematsu S, Takeuchi O. Pathogen recognition and innate immunity. *Cell*. 2006;124(4):783–801. doi:10.1016/j.cell.2006.02.015
36. Christmas P. Toll-like receptors: sensors that detect infection. *Nat Educ*. 2010;3(9):85.
37. Sun J, Li N, Oh K-S, et al. Comprehensive RNAi-based screening of human and mouse TLR pathways identifies species-specific preferences in signaling protein use. *Sci Signaling*. 2016;9(409):ra3–ra3. doi:10.1126/scisignal.aab2191
38. Liew FY, Xu D, Brint EK, O'Neill LA. Negative regulation of toll-like receptor-mediated immune responses. *Nat Rev Immunol*. 2005;5 (6):446–458. doi:10.1038/nri1630
39. Negishi H, Ohba Y, Yanai H, et al. Negative regulation of Toll-like-receptor signaling by IRF-4. *Proc Natl Acad Sci*. 2005;102(44):15989–15994. doi:10.1073/pnas.0508327102
40. Hu Y-H, Wang Y, Wang F, et al. SPOP negatively regulates toll-like receptor-induced inflammation by disrupting MyD88 self-association. *Cell Mol Immunol*. 2021;18(7):1708–1717. doi:10.1038/s41423-020-0411-1
41. Wang J, Hu Y, Deng WW, Sun B. Negative regulation of toll-like receptor signaling pathway. *Microb Infect*. 2009;11(3):321–327. doi:10.1016/j.micinf.2008.12.011
42. Dias ML, O'Connor KM, Dempsey EM, O'Halloran KD, McDonald FB. Targeting the Toll-like receptor pathway as a therapeutic strategy for neonatal infection. *Am J Physiol Regul Integr Comp Physiol*. 2021;321(6):R879–R902. doi:10.1152/ajpregu.00307.2020
43. Newman RM, Salunkhe P, Godzik A, Reed JC. Identification and characterization of a novel bacterial virulence factor that shares homology with mammalian toll/interleukin-1 receptor family proteins. *Infect Immun*. 2006;74(1):594–601. doi:10.1128/IAI.74.1.594-601.2006
44. Arpaia N, Barton GM. The impact of toll-like receptors on bacterial virulence strategies. *Curr Opin Microbiol*. 2013;16(1):17–22. doi:10.1016/j.mib.2012.11.004
45. Jiang D, Liang J, Fan J, et al. Regulation of lung injury and repair by Toll-like receptors and hyaluronan. *Cell Mol Life Sci*. 2005;11(11):1173–1179.
46. Huang M, Cai S, Su J. The pathogenesis of sepsis and potential therapeutic targets. *Int J Mol Sci*. 2019;20(21):5376. doi:10.3390/ijms20215376
47. van der Poll T, Shankar-Hari M, Wiersinga WJ. The immunology of sepsis. *Immunity*. 2021;54(11):2450–2464. doi:10.1016/j.immuni.2021.10.012
48. Zuany-Amorim C, Hastewell J, Walker C. Toll-like receptors as potential therapeutic targets for multiple diseases. *Nat Rev Drug Discov*. 2002;1 (10):797–807. doi:10.1038/nrd914
49. Hennessy EJ, Parker AE, O'neill LA. Targeting toll-like receptors: emerging therapeutics? *Nat Rev Drug Discov*. 2010;9(4):293–307. doi:10.1038/nrd3203
50. Zaman R, Islam RA, Ibnat N, et al. Current strategies in extending half-lives of therapeutic proteins. *J Control Release*. 2019;301:176–189. doi:10.1016/j.jconrel.2019.02.016
51. Piao W, Ru LW, Piepenbrink KH, Sundberg EJ, Vogel SN, Toshchakov VY. Recruitment of TLR adapter TRIF to TLR4 signaling complex is mediated by the second helical region of TRIF TIR domain. *Proc Natl Acad Sci USA*. 2013;110(47):19036–19041. doi:10.1073/pnas.1313575110
52. Piao W, Vogel SN, Toshchakov VY. Inhibition of TLR4 signaling by TRAM-derived decoy peptides in vitro and in vivo. *J Immunol*. 2013;190 (5):2263–2272. doi:10.4049/jimmunol.1202703
53. Fosgerau K, Hoffmann T. Peptide therapeutics: current status and future directions. *Drug Discov Today*. 2015;20(1):122–128. doi:10.1016/j.drudis.2014.10.003
54. Cleal K, He L,D, Watson P,T, Jones A. Endocytosis, intracellular traffic and fate of cell penetrating peptide based conjugates and nanoparticles. *Curr Pharm Des*. 2013;19(16):2878–2894. doi:10.2174/1381612813199990297
55. Hamm-Alvarez SF, Sonee M, Loran-Goss K, Shen W-C. Paclitaxel and nocodazole differentially alter endocytosis in cultured cells. *Pharm Res*. 1996;13:1647–1656. doi:10.1023/A:1016432505275
56. Sakai T, Yamashina S, Ohnishi S-I. Microtubule-disrupting drugs blocked delivery of endocytosed transferrin to the cytocenter, but did not affect return of transferrin to plasma membrane. *J Biochem*. 1991;109(4):528–533. doi:10.1093/oxfordjournals.jbchem.a123415
57. Wang D, Zeng Z, Shen M, et al. ATP consumption is coupled with endocytosis in exudated neutrophils. *Int J Mol Sci*. 2023;24(10):9039. doi:10.3390/ijms24109039
58. Schmid SL, Carter LL. ATP is required for receptor-mediated endocytosis in intact cells. *J Cell Biol*. 1990;111(6):2307–2318. doi:10.1083/jcb.111.6.2307

59. Blaser H, Dostert C, Mak TW, Brenner D. TNF and ROS crosstalk in inflammation. *Trends Cell Biol*. 2016;26(4):249–261. doi:10.1016/j.tcb.2015.12.002
60. Magnez R, Bailly C. Microscale thermophoresis as a tool to study protein interactions and their implication in human diseases. *Int J Mol Sci*. 2022;23(14):7672. doi:10.3390/ijms23147672
61. Romain M, Thiroux B, Tardy M, Quesnel B, Thuru X. Measurement of protein-protein interactions through microscale thermophoresis (MST). *Int J Mol Sci*. 2020;10(7):e3574.
62. Jerabek-Willemsen M, Wienken CJ, Braun D, Baaske P, Duhr S. Molecular interaction studies using microscale thermophoresis. *Nat Commun*. 2011;9(4):342–353.
63. Liu L, Lucas RM, Nanson JD, et al. The transmembrane adapter SCIMP recruits tyrosine kinase Syk to phosphorylate toll-like receptors to mediate selective inflammatory outputs. *J Biol Chem*. 2022;298(5):101857. doi:10.1016/j.jbc.2022.101857
64. Tang N, Tian W, Ma GY, et al. TRPC channels blockade abolishes endotoxemic cardiac dysfunction by hampering intracellular inflammation and Ca(2+) leakage. *Nat Commun*. 2022;13(1):7455. doi:10.1038/s41467-022-35242-0
65. Splith K, Neundorf I. Antimicrobial peptides with cell-penetrating peptide properties and vice versa. *Eur Biophys J*. 2011;40(4):387–397. doi:10.1007/s00249-011-0682-7